SISSA - SCUOLA
INTERNAZIONALE
SUPERIORE
DI STUDI AVANZATI
TRIESTE
Strada Costiera 11

ISAS - INTERNATIONAL SCHOOL FOR ADVANCED STUDIES

October 1984

SPIRAL GALAXIES AND THEIR ROTATION CURVES

Thesis submitted for the degree

of

Master of Philosophy

CANDIDATE:

P.Salucci

SUPERVISOR:

Prof. D.W.Sciama

TRIESTE

INDEX

INTRODUCTION

One of the most important events for understanding the Universe duning past $\sim$ 5 years has been the realization,both theoretical and observative,that large fraction of total mass $\sim$ 90 % is in very low luminous and almost surely non barionic form:gas and star can't account for the inferred mass.

That has been leading the interest of many astronomers, cosmologists,and elementary particle phisicists,and there is not far the possibility that "astronomy can probe SUSY" or someother theory of fundamental interactions.

Nevertheless,despite the fact that the "missing mass" problem was borne by analysis of rotation curves in the late seventies,very few interrelations,between this new idea and old problems in understanding dynamics and morphology of spirals have been developed.

The picture is:within R_{25} radius 40 % of mass is in non barionic spherically distribuited form; 60 % is in the disc.

Some interrelations are easy to imagine: halo stabilizes disc and helps to transfer angular momentum.

Before continuing,it is necessary to stress that from

its links with axisymmetric structure and dynamics (Chapter III);in chapter IV we present some preliminar results showing that our point of view is an interesting starting point.

Note that in the review we stress when we run into any old, and supposed working pictures or models that don't (or partially) match with the dark haloes idea.

Before studying internal kinematics and dynamics,we briefly describe the morphology of spiral galaxies.

We are going to do it not only in order to know what we are talking about,but also because we think that,behind the various features the galaxies appear with,there is involved a lot of phisics.

Morphology is an often qualitative,rough and quite dependent on the observer study of galaxies;(for example:generations of astronomers have been insisting on believing that Nature must follow their discrete classifications;if an object tries to rebel,it comes a (bad)fenomenum ready for a further list).

Nevertheless we think that today this is the best kind of knowledge we have about disc galaxies.

Impressive features are often the visible manifestation through bad known mechanism of bad known interactions among unknown components forming galaxies.

Disc galaxies bifurcate in two branches:normal and barred,SA,SB,occurring with similar frequency;this classification is not unambiguous,most of galaxies show some of the characteristics of barred galaxies and only the more extreme examples are classified as barred.

In part this ambiguity comes out because we don't know if the bar is a permanent feature existing if some initial con-

ditions are present,or it is a temporary stage during the evolution of a galaxy.

At the junction of the elliptical and the spiral it comes out the lenticular classe designed as S0 or SB0 according to the presence of the bar.

Lenticulars are disc galaxies with a central bulge,but the disc component is structureless.

Between sferoidal region and outer parts many lenticulars possess smooth features called lenses.

A normal spiral has a brightness condensation located at the center of a thin disc containing spiral arms;itsshape and the globality of the pattern vary from one galaxy to an other; they also vary following the Hubble-De Vancoulers sequence $a \to b \to c \to d$ fig 1.

The barred spirals have a star bar,interior to the generally two-arms structure which appear to be sheared by the bar itself.

Within each class of spiral,normal a barred,we have a sequence of sub-types,according to a combination of many criteria (Table 1),slightly different for each of the classification scheme in the literature.
Some of galaxies,both SA and SB,have one or more rings,or a S-shaped structure.

FIG 1

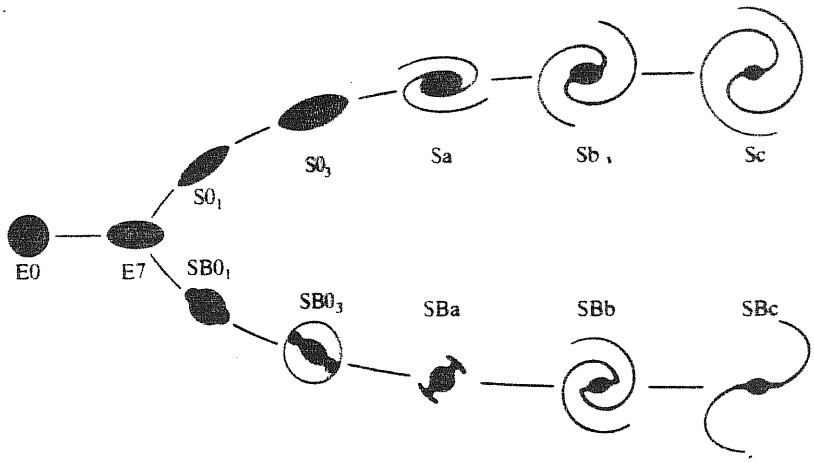

The Hubble tuning-fork diagram. The diagram shown here differs from Hubble's original in that it shows various stages of lenticular galaxies interposed between the ellipticals and the spirals.

Frequencies of Main Classes

Class	E	SO	S	Im	IO	Pec
f (per cent)	13.0	21.5	61.1	2.55	0.85	0.9

Frequencies of Subtypes among 994 Spiral Galaxies

	O/a	a	ab	b	bc	c	cd	d	dm	m	?	Total	f
SA	17	25	25	57	57	82	30	9	3	4	2	311	31.3
SAB	13	15	23	45	50	71	35	11	3	7	1	274	27.6
SB	26	43	33	83	27	55	27	28	9	30	10	366	36.8
S	4	1	-	6	1	13	1	10	-	-	7	43	4.3

TABLE 1

System	Principal criteria	Symbols employed	Examples of classifications
Hubble-Sandage	barrishness; openness of arms/disk-bulge ratio; degree of resolution of arms into stars	E, S0, S, SB, Ir a, b, c	M87 = E1 M31 = Sb M101 = Sc LMC = Irr I
de Vaucouleurs	barrishness; openness of arms/disk-bulge ratio; ring or *s* shapes	E, S0, S, SA, SB, I a, b, c, d, m, (r), (s)	M87 = E1P M31 = SA(s)b M101 = SAB(rs)cd LMC = SB(s)c
Yerkes	central condensation of light; barrishness/smoothness	k, g, f, a E, R, D, S, B, I	M87 = kE1 M31 = kS5 M101 = fS1 LMC = afI2
Revised DDO	young-star richness of disk; barrishness; central concentration of light; quality and length of arms	E, S0, A, S, Ir B a, b, c I, . . . , V	M87 = E1 M31 = Sb I–II M101 = Sc I LMC = Ir III–IV

Disk and Bulge Parameters for Spiral and Lenticular Galaxies

NGC	Type	$-M_B$	r_s/kpc	B_s/μ_B	r_e/kpc	B_e/μ_B	D/B
3384	S0	20.4	3.9	22.13	1.2	20.51	0.7
4270	S0	20.3	3.1	21.36	2.7	22.49	1.0
4281	S0	21.2	4.4	20.93	1.1	19.71	1.6
4459	S0	20.6	3.7	22.19	3.7	22.19	0.2
4526	S0	21.3	6.9	22.10	4.8	22.41	0.7
4570	S0	20.2	2.5	20.78	0.4	18.98	1.8
224 (M31)	Sb	19.8	4.5	21.4	3.5	17.5	3.2
598 (M33)	Sc	17.8	1.4	21.4	<0.5	–	>12

Then SAc(r) means a normal spiral galaxy, with spiral structure well pronounced possessing a ring, and SBb(s) means a barred galaxy S -shaped with two-armed global spiral structure.

Fotometry of spiral galaxies:

The brightness distribution of spiral galaxies is very complex: in addition to the central bulge elliptical-like component, to the disk component and to the Pop II star halo component (corona), we have bar, lens and spiral structures which complicate considerably the brightness distribution .

The disk component has surface brightness : [25]

$$\sigma_D = \sigma_S \, e^{-R/R_S} \qquad (1.1)$$

The bulge component follows the so called De Vancoulers $r^{1/4}$ law

$$\sigma_B = \sigma_e \, e^{-7.67\left[(R/R_e)^{1/4} - 1\right]} \qquad (1.2)$$

For the total luminosity we have :

$$\frac{L_D}{L_B} \simeq 0.28 \left(\frac{R_S}{R_e}\right) \frac{\sigma_S}{\sigma_e} \qquad (1.3)$$

This ratio increases from Sa to Sc types.

The spiral structure can be seen by fotometry plotting brightness profiles (fig. 2) versus azimuthal angle θ.

The underlying disk is found very uniform and rather red $(B-V) \simeq 0.75 \pm 0.05$.

The arms are seen in the U, B and sharper in the orange

FIGURE 2A

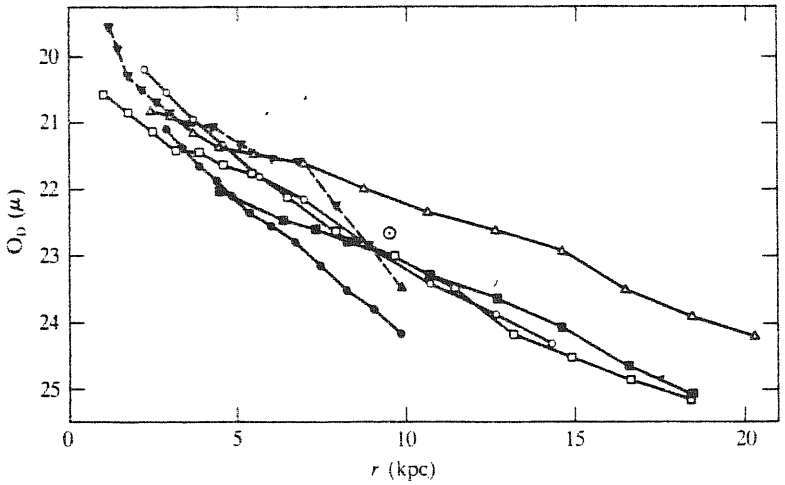

Orange surface brightness versus radius for six spiral galaxies [NGC 3031 (●), NGC 4255 (○), NGC 4321 (△), NGC 5194 (▼), NGC 5364 (■), and NGC 5457 (□)]. The solar symbol ⊙ indicates the estimated surface brightness of our Galaxy near the Sun. Notice that the outer parts of the profiles tend to be fairly straight in accord with equation (5-6)

FIGURE 3

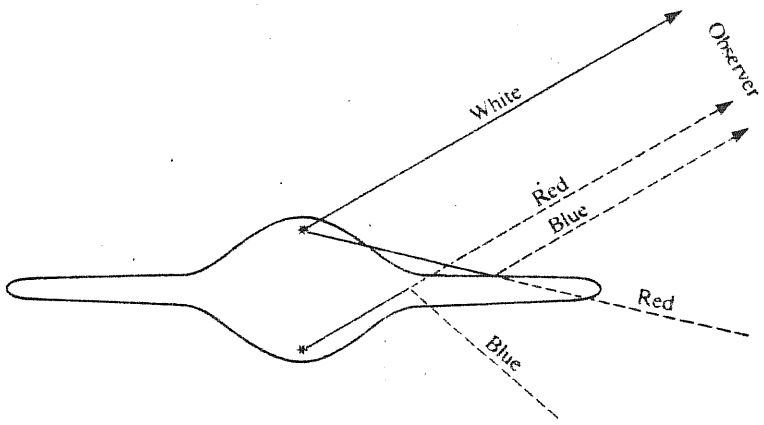

Effects of scattering and absorption of light by dust on the images of disk galaxies. Light from the top of the bulge reaches the observer without obstruction by dust in the disk. Light from the lower portion of the bulge is partially absorbed by the disk. Some light is forward scattered by the disk into the path to the observer.

FIGURE 2B

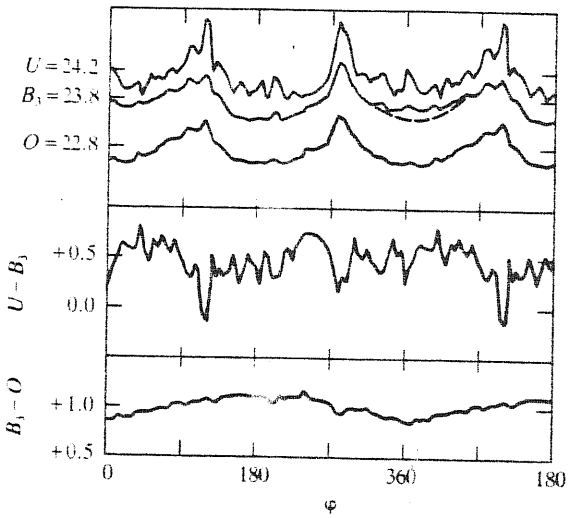

Spiral structure in M81. U, B, and O azimuthal profiles at $r = 475$ arcsec. The angle ϕ is measured from the apparent major axis in the direction of rotation. The profile has been continued periodically beyond $\phi = 360°$. Notice how the U profile consists of narrow peaks superposed on a broader wave pattern which resembles the B and O profiles.

passband, where the brightness due to arms is 50% of the axisymmetric disk. FIG 2B.

The arms are so brilliant because massive stars born and die there; besides along arms (near maxima of spiral gravitational field) like a pearl necklace there are giant H II regions formed through shock-waves propagating in the gaseous disk.

Dust scatters light and absorbes it; that leads to color and brightenss asymmetries between the far and near sides of disk galaxies (fig. 3)

It is possible from fotometry to obtain a standard diameter $R_{25} \equiv R_{dV}$ of a galaxy R_{25} is the diameter (in *arcmin*) that the 25 *mag arcsec*$^{-2}$ contour would have if the galaxy were seen face on and were unobscured by dust.

In the disk galaxies differential rotation opposes to gravity to build up stable systems.

In first approximation we can assume:

1) disk galaxies are collisionless star systems, infact: a) gas content, $\sim 10\%$ in mass, is negligible b) the typical star-star relaxation time τ is much longer of the age of the Universe $\tau H_0^{-1} \gg 1$.

2) The underlying gravitational field is axisymmetric: $\Phi = \Phi(R,z)$ it reflects the axisymmetric stationary distribution of mass.

The impressive not-axisymmetric features, bars and spiral structures, are only the wonderful and spectacular manifestation of a (perturbative) weak not-axisymmetric field.

With assumption (1), (2) total mass $\mathcal{M}$, surface density μ, gravitational field in the plane of the galaxy Φ have obtained balancing the centrifugal acceleration with the gravitational attraction

$$v^2 = R \left(\frac{\partial \Phi}{\partial R}\right)_{z=0} \qquad (2.1)$$

and using Poisson equation to link density with gravitational field (or better mass with geometry)

$$\nabla^2 \Phi = 4\pi G \rho \qquad (2.2)$$

The (2.1) (2.2) deserve some comments:

1) Though the not circular velocities are generally small and there

fore (2) is true, we have to realize that the measured rotational velocity $V_{obs}(R)$ is quite biased by not-circular velocities $V_1(R)$ involved with bar-like or spiral-like perturbative gravitational fields:

$$V(R) = V_{obs}(R) - V_1(R) \qquad (2.3)$$

w

$$\frac{\langle V_1 \rangle}{\langle V \rangle}\Big| \leq 0.05 \quad \text{averaged within all the galaxy} \qquad \text{but} \quad \frac{V_1}{V}\Big| \sim 0.2 \quad \text{Across the arms.} \qquad (2.4)$$

Because we have as typical values

$$V \sim 250 \ \text{Km s}^{-1} \qquad V_1 \sim 50 \ \text{Km s}^{-1} \qquad (2.5)$$

$$\left|\frac{dV}{dR}\right| \sim 1 \ \text{Km s}^{-1}\text{Kpc}^{-1} \qquad \left|\frac{dV_1}{dR}\right| \sim 20 \ \text{Km s}^{-1}\text{Kpc}^{-1}$$

We see that a not-axisymmetric gravitational field affects moderately the observational velocity field, nevertheless it biases so completely the derivative that we must take away the contribute of perturbations from velocity field before computing it to have the actual derivative of the circular velocity involved with the axisymmetric gravitational field.

2) The observative velocity is measured in the (projected) frame of the plan of sky that coincides with the plan of the galaxy only when the galaxy is face-on ($i = 90$)

Otherwise, the transformation laws from the plan of the sky to plan of the galaxy are:

$$R = s\left[\sec^2 i - tg^2 i \cos^2\eta\right]^{1/2}$$

$$V = V_{SKY}\frac{\left[\sec^2 i - tg^2 i \cos^2\eta\right]^{1/2}}{\sin i \cos\eta} \qquad (2.6)$$

Where s is radial distance in the plane of the sky, i is inclination angle and η is the angle between $\vec{s}$ andthe direction of the major semiaxis.

We note that is not sufficient to have good spettroscopic measures, (i. e. in the plane of the sky), to have good rotation curves: we also need the actual value of inclination angle i from kinematics or from fotometry; in some case, small galaxy with big bulge, i is known badly causing large uncertainties in V .

INFINITELY THIN DISK MODEL

The (2.1) (2.2) with the idealization of a distribution of matter within highly (infinitely) flattened disk, have a simple analitical solution.

We start espressing the surface densit $\mu(R)$ as a Beessel integral [14]

$$\mu(R) = \int_0^\infty J_0(KR)\, K\, S(K)\, dK$$
$$S(K) = \int_0^\infty J_0(KR)\, u\, \mu(u)\, du \qquad (2.7)$$

then the potential is [14]

$$\phi(R,Z) = 2\pi G \int_0^\infty J_1(KR)\, S(K)\, e^{-K|Z|}\, dK \qquad (2.8)$$

because

$$\mu(R) = -(2\pi G)^{-1} \left[\frac{\partial \phi}{\partial z}\right]_{z=0+} \qquad (2.9)$$

We can also express V^2/R as integral

$$V^2/R = \int_0^\infty J_1(KR)\, K \int_0^\infty V^2(u)\, J_1(Ku)\, du\, dK \qquad (2.10)$$

Now we use the typical radial disk distribution of surface brightness I(R) [25].

$$I(R) = I_0\, e^{-\alpha R} \qquad (2.11)$$

Where α^{-1} is a typical luminous lenght of the disk

$$2\ \text{Kpc} \leq \alpha^{-1} \leq 6\ \text{Kpc} \qquad (2.12)$$

It is reasonable [25] to assume that (2.12) implies a surface-density distribution :

$$\mu(R) = \mu_0\, e^{-\alpha R} \qquad (2.13)$$

Therefore we obtain from (2.7) (2.8) (2.10) (2.13)

$$V^2(R) = \pi G \mu_0 \alpha R^2 \left(I_0\left(\tfrac{1}{2}\alpha R\right) K_0\left(\tfrac{1}{2}\alpha R\right) - I_1\left(\tfrac{1}{2}\alpha R\right) K_1\left(\tfrac{1}{2}\alpha R\right) \right) \qquad (2.14$$

I,K, are modified Bessel functions

Then, the total mass is

$$m = 2\pi\mu_0 a^2 \qquad (2.15)$$

Then inserting (2.14) (2.13) in (2.7) we find

$$S(K) = (2\pi G)^{-1} \int_{K=0}^{\infty} V^2(u)\, J_1(Ku)\, du$$

$$\mu(R) = (2\pi G)^{-1} \int_{K=0}^{\infty} J_0(KR)\, K \int_{u=0}^{\infty} V^2(u)\, J_1(Ku)\, du\, dK \qquad (2.16)$$

and with the boundary conditions $V(0) = V(\infty) = 0$

$$\mu(R) = (2\pi G)^{-1} \int_{u=0}^{\infty} \frac{dV^2}{du} H(u,R)\, du \qquad (2.17)$$

$$H(u,R) = \frac{2}{\pi R} K\left(\frac{u}{R}\right) \qquad u < R$$

$$= \frac{2}{\pi u} K\left(\frac{R}{u}\right) \qquad u > R$$

K is the first complete elliptic integral.

A rough approximation of (2.17) is [14]

$$\mu(R) = \mu(0) + (2\pi G)^{-1} \left[0.39 \frac{d}{dR} - \int_0^R \frac{V^2(u)}{u^2} du \right. \qquad (2.18)$$

Therefore we obtain the surface density from rotation velocity.

We can write (2.14) in dimensionless form, let $\hat{R} = \alpha R$ and $\hat{V} = V/(GM\alpha)^{1/2}$

then

$$\hat{V}^2(\hat{R}) = \frac{1}{2} \hat{R}^2 \left[I_0\left(\tfrac{1}{2}\hat{R}\right) K_0\left(\tfrac{1}{2}\hat{R}\right) - I_1\left(\tfrac{1}{2}\hat{R}\right) K_1\left(\tfrac{1}{2}\hat{R}\right) \right] \qquad (2.19)$$

This rotation curve is shown in figure [4]

In has a maximum velocity, $\hat{V} \simeq 0.62$ at $\hat{R} \simeq 2$ then it

FIGURE 4

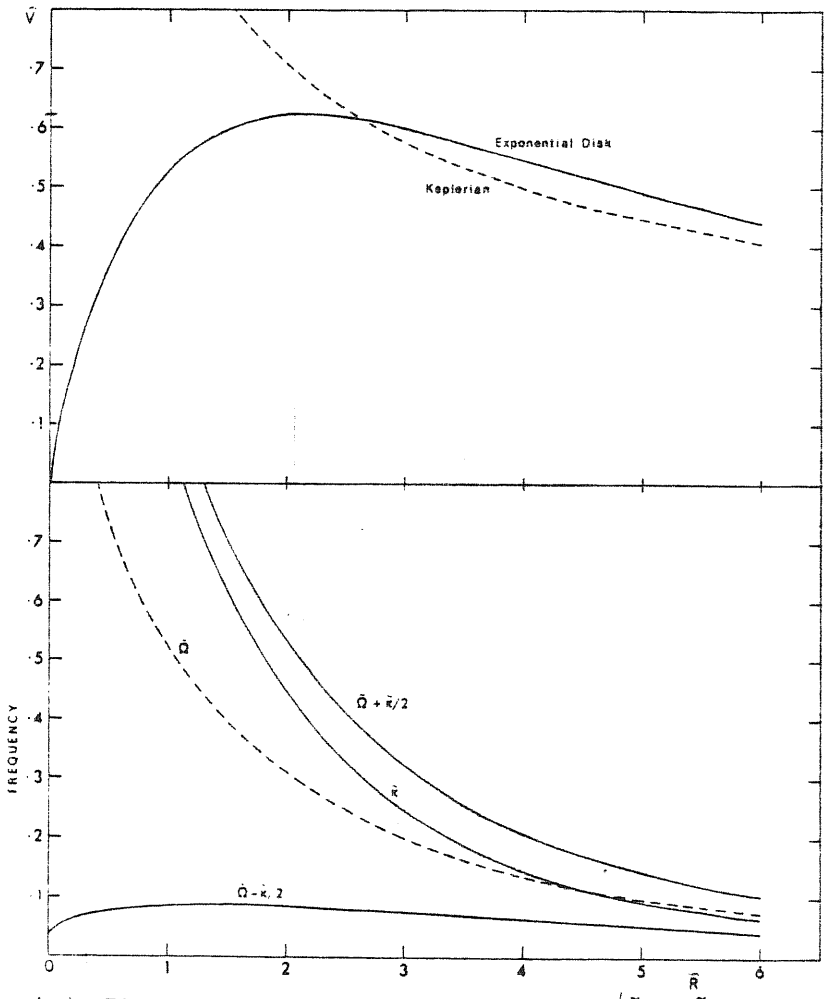

(*top*).—Dimensionless rotation curve for the exponential disk. ($\tilde{V}$ and $\tilde{R}$ are defined in the text) Broken line shows the corresponding Keplerian curve.

(*bottom*).—Dimensionless angular velocity, epicyclic frequency, and Lindblad-resonance frequencies for the exponential disk

decreases outwards.

This decrease, though clear, is moderate: when the star disk is supposed to be finished the velocity is $\sim 0.7\,\hat{V}_{MAX}$ (we note that from star lines spettroscopy this decrease would be scarcely observable); nevertheless let us stress that we are talking about distances $< 6\alpha^{-1} \simeq 10\text{-}20$ Kpc: matter (gas) found well outside the star disk ~ 40 Kpc, following (2.19), must present large decrease of velocity.

The infinitely thin disk model is attractive because from the fotometric quantity α^{-1} and dynamical quantity $\hat{V}_{MAX}$, it is possible to work out the rotation velocity, total mass, mass distribution and total angular momentum; infact in addition to (2.14)(2.18) we have that the m inside $\hat{R}$ is

$$m(\hat{R}) = m\left[1 - e^{-\hat{R}} - \hat{R}\,e^{-\hat{R}}\right] \qquad (2.20)$$

and the total angular momentum is

$$H = (G m^3 \alpha^{-1})^{1/2} \propto m^{3/4} \qquad (2.21)$$

We conclude this section stressing again that the exponential disk model implies:

$$V(R) \simeq V(R_{MAX}) \qquad \frac{R}{R_{MAX}} \leq 2 \qquad (2.22)$$

$$V(R) \simeq V(R_{MAX}) \qquad \frac{R}{R_{MAX}} \simeq 10$$

but, unfortunately when $R \simeq 10\,R_{MAX}$ star disk is undetectable.

Spherical model

As we will see in the 3° chapter, recent 21 cm observational velocities are consistent with a spherical isothermal distribution of mass:

$V \sim \text{CONST}$ $\qquad \rho \propto r^{-2}$ (Spherical coordinates r, θ, ϕ).

It comes out that, roughly speaking, whitin each galaxy the rotational velocity is a constant, decreasing from early to late morphological types. Then modelling galaxies as spheres we easily get:

$$\begin{aligned} m &= G^{-1} V^2 R \\ j &= V R \\ \frac{j}{M} &= G V^{-1} \mathcal{L} m^{-1/2} R^{1/2} \end{aligned} \qquad (2.23)$$

This important fact means:

1) though the thin disk model sounds reasonable: the distribution of luminous matter is highly flattened: thickness of star + gas disk $\lesssim 1$ Kpc the internal kinematics excludes it: we find $V(20\, R_H) \simeq V(R_H)$ for all galaxies (~ 100) whose rotation curves are studied .

2) observations imply that consistent fraction ($\sim 50\%$) of the mass within R_{25}, is spherically distribuited in subluminous or non-luminous form.

3) Nevertheless the disk is responsable for the remaining 50% of the mass within R_{25}

1), 2) and 3) introduce us in the galactic conspiracy problem.

We find that at least three component build up a spiral galaxy: a star

disk and a probabily ellipsoidal star halo, detected by the fotometry, and a low (non) luminous halo, inferred by the dynamics. Unfortunately all three component mix each other to simulate perfectly just one spherical isothermal component.

In other words the inner regions of galaxies are disk-dominated, the outer one are halo dominate: the transition zone should be clearly visible, as we see the bulge-disk transition zone, but no track is present in rotation curves.

DISK + HALO MODELS

We think that, considering flatness of rotation curves as turning effect of different components, an improvement is to develop multicomponent models of galaxies. [30]

We start with a thin disc with a surface density profiles $\mu_D(R)$ and circular velocity $V_D(R)$ embedded in a spherical halo with a density $\varrho_H(r)$ where $r^2 = R^2 + z^2$

The matter in the disk rotates in centrifugal balance:

$$V_D^2/R = -a_D(R) - a_H(R)$$

a_D and a_H : radial components of acceleration in the equatorial plane arising separately from the mass distribution in the disc and halo.

$$a_D = -2\pi G \int_0^\infty dK\, K\, J_1(KR) \int_0^\infty dz'\, z'\, J_0(Kz')\, \mu_D(z')$$

$$a_H = -4\pi G R^{-2} \int_0^r dz\, r^2\, \varrho_H(r)$$

... we get the density profile of the halo in terms of properties of the disk.

$$\varrho_H(r) = -\frac{1}{4\pi G r^2} \frac{d}{dr}\left\{ r^2 \left[a_D(r) + V_D^2(r)/r \right] \right\} \qquad (2.2\ )$$

The total mass and angular momentum are:

$$M_D = \int_0^\infty 2\pi R\, \mu_D\, dR \qquad (2.25)$$

$$M_H = \int_0^\infty 4\pi r^2 \varrho_H(r)\, dr \qquad (2.26)$$

$$J_D = \int_0^\infty 2\pi R \mu_D(R) R V_D(R) dR \qquad (2.27)$$

$$J_H = \int_0^\infty \mu_H(R) R^2 V_H(R) dR \qquad (2.28)$$

where

$$\mu_H = 2\int_0^\infty dz \, \varrho_H(z) [R^2 + z^2]^{1/2} \qquad (2.29)$$

is the surface density of the halo proiected on the plane of the disk.

The (2.24/28) are a good starting point to study the disk-halo model.

Even if we use in the (2.25) the exponential model surface density

$$\mu_D = \left(\frac{\alpha^2 m_D}{2\pi}\right) e^{-\alpha R} \qquad (2.30)$$

the system (2.24/28) is not closed yet: to solve it we need phisical assumption leading relationship among quantities involved.

For istance in the Fall-Efstation picture disc galaxies formed from collaping star in extended haloes of dark material; it is assumed that these systems were producted by hierarchical clustering and acquired their angular momenta by tidal

In this picture it is aspected

$$J_D/m_D = J_H/m_H \qquad (2.31)$$

and because each element of material in the disc conserves its angular momentum from the time it begins to collapse

$$m_D(j)/m_D = m_H(j)/m_H \qquad (2.32)$$

where $m(j)$ is the mass whitin the radius j/V ($j = VR$ is the specific angular momentum).

Moreover from N- Body experiments [10] the general condition for stability of relatively cold disc against low order modes (bar-like) is

$$t \simeq \frac{1}{2}(1+f_c)^{-1} \leq 0.14 \qquad (2.33)$$

here

$$f_c \equiv \frac{\text{Potential energy stored in the disk-Halo interaction}}{\text{Potential energy stored in the self attraction of the disk}}$$

$$= \frac{\int_0^\infty dR\, R\, \mu_D R\, a_H(R)}{\int_0^\infty dR\, R\, \mu_D R\, a_D(R)} \qquad (2.34)$$

Finally, they use a rotational velocity $V_D(R)$ which follow the exponential disc model in the inner region and a Keplerian rotation curve at R greater than R_t a cut-off radius.

$$V_D = V_m \left(\frac{R^2}{R_m^2+R^2}\right)\left[1+\gamma \ln\left(\frac{R^2}{R_m^2+R^2}\right)\right]^{1/2} \qquad (2.35)$$

where V_m and R_m are parameter and γ must be $= \left(\frac{1}{2}\alpha R_m\right)^2 \left(\alpha m_D G V_m^2\right)$ to avoid an infinite central density of the halo.

So it is possible to obtain a rotation velocity which keeps constant for $0.1 \lesssim R/R_t \lesssim 1$ fig. [5] and the model tested with observations seem to have a good self consistence.

We have described this model just to present an exemple of solution of (224) (225) (228) by means of a phisical model (gravitational clustering, in facts we think that a cut-off radius and finite central density should come out from the theory and not to be the starting point;

we are going to use the observational rotational velocity V instead the ad hoc formula (235) to specify the rotational velocity of disc matter.

EPICYCLE ORBITS

In cylindrical coordinate R, θ, z the equation of motion for a star in an axisymmetric gravitational field may be written

$$\begin{aligned} \ddot{R} &= R\dot{\theta}^2 - \frac{\partial \phi}{\partial R} \\ R\ddot{\theta} &= -2\dot{\theta}\dot{R} \\ \ddot{z} &= -\frac{\partial \phi}{\partial z} \end{aligned} \qquad (2.36)$$

The second equation gives $j = R^2\dot{\theta}$

We refer the orbit of a star to a almost circular reference orbit situated in the plane of symmetry of the potential .

let us write : $R = R_0 + \xi \quad , z = \delta z \qquad R_0 = \text{const.}$

Under the assumptions

$$\frac{\xi}{R_0} \simeq \frac{dz}{R_0} << \left[\frac{1}{\phi}\frac{d\phi}{dR}\right]^{-1} \qquad (2.37)$$

$$\frac{R_0}{} << 1$$

$$\ddot{\xi} = -\left[\frac{3}{R_0}\left(\frac{\partial \phi}{\partial R}\right)_0 + \frac{\partial^2 \phi}{\partial R^2}\right]\xi \qquad (2.38)$$

$$\delta\ddot{z} = -\left[\frac{\partial^2 \phi}{\partial z^2}\right]_0 \delta z$$

We set : $\left[\frac{3}{R_0}\left(\frac{\partial \phi}{\partial R}\right)_0 + \left(\frac{\partial^2 \phi}{\partial R}\right)_0\right] = 4\Omega^2\left[1 + \frac{1}{2}\frac{\partial \ln \Omega}{\partial \ln R}\right] = \kappa^2 \qquad (2.39)$

Then the orbit will follow a periodical path both in the R and Z direction :

$$\begin{aligned} \xi &= a \sin(\kappa(t - t_1)) \\ \delta z &= b \sin(\lambda(t - t_2)) \end{aligned} \qquad (2.40)$$

$$\lambda = \left(\frac{\partial^2 \phi}{\partial z^2}\right)_0^{1/2}$$

The radial displacement will cause a tangential dispacement affecting the phase Θ by a quantity η

$$\eta = \left(\frac{2\Omega}{K}\right)\frac{a}{R}\cos[K(t-c_1)] \qquad (2.41)$$

$$a = \frac{\Pi}{K} \quad \text{if at} \quad t=t_1,\ R\dot{\Theta} = \Pi$$

Then the orbit has a (2+1) geometry: obscillations with respect to galactic plane in the azimuthal direction and, in the plane of the galaxy, superposition of elliptical orbit of major axis on a circular one of radius R_0 with $\frac{a}{R_0} << 1$

$$R = R_0 + \frac{\Pi}{K}\sin Kt \qquad (2.42)$$

$$\Theta = \Omega t + \frac{1}{R_0}\left(\frac{2\Omega}{K}\right)\left(\frac{\Pi}{K}\right)\cos Kt$$

Most of individual orbits far from the bar or spiral arm satisfy (2.42) and they can described from the epicycle approximation.

Nevertheless some star, by scattering with not-axisymmetric potential or with giant molecolar clouds, can acquire large amount of energy in not-circular motions settling up in a peculiar orbit.

ROTATION CURVES DATA

The starting point for any dynamical study of galaxy is the analisis of rotation curves.

We show in fig. (6) (7) and in table (2) pratically all curve we have whose $R_{farthest}$ is comparable with R_{25} and well outward R_{25}

Most of these are due to Rubin and C. [11] [31] (we owe thank to her because she kindly sent to us some Sa unpublieshed curves), a part to Bosma,

Before any comment, we stress the unfortunate tendency

of presenting data obtained in plotted form without any table: we know data for 650 galaxies, in the 75% of them, chiefly in the old literature, it is hard to infer the value of $V(R)$.

It is important to note that following (2.6) we have to know the inclination of a galaxy very well to have the true value of V in the plan of the galaxy, that is serius when $i \to 0$, the error is infacts

$$\Delta V \propto \Delta i \; tg(90-i) \qquad (2.43)$$

We know i or from kinematics or from photometry, but in both case we find difficulties for some Sa galaxies where $\frac{D}{B} \sim 1$: the inclination obtained so is that of the spheroidal component not necessarily equal to that of the disk component an exemple NGC 4800

A first look of curves of table (2) tells us that no one of them follows the "classical" falling profiles; all can be considered flat or sligh

TAV. 2

	<Radius> (kpc)																									
	0.5	1.0	1.5	2.1	3	4	5	6	7	8.2	10	12	14	16	18	20	22	24	26	30	35	40	46	56	70	82
Sa																										
NGC 1023	11±8(0.02)	117	204	171±88	205±31	236	...	...	...	...	260±7	261±4	254±4	250±4	242±4	...	...	...	...	...	237±10	221±7	216±6	131±1	155±8	NO!
NGC 1357	...	...	170±20	209±24	248±8	212±13	219±13	235±4	265±5	267±13	252±12	259±5														
NGC 2639	...	...	...	...	179±3	249±7	286±4	309±4	318±4	318±3	323±2	319±4	318±4	330±4												
NGC 2775	...	...	...	...	253	269±5	272±6	289±2	303±4	284±2	291±5	270±4	NO													
NGC 2844	6(0.01)	85±4	113±4	137±2	153±5	160±4	141±4	153±3	148±10	171																
NGC 3351	...	...	...	...	182	199±5	191±8	186±3	187±12	184	209±12	203±10	226													
NGC 3593	27±5(0.11)	65±3	108±4	110±4	101±4																					
NGC 3898	...	166	147±30	205	198	207±4	211±1	219	240±5	240±5	249±4	259±3	248±5	260±12												
NGC 4378	...	207±26	201±9	314±21	327±21	317±19	316±10	319±10	309	...	...	308±1	329±43	251	286±13	300	288±2	271								
NGC 4419	-3±7(0)	88±6	124±8	150±9	169±2	177±3	187±3																			
NGC 4594	201±16(0.38)	97±16(0.78)	94±12	105±13	176±7	259±7	334±9	322±8	331±6	340±9	304±3	329±6	359±9	365±3	365±2											
NGC 4698	...	57	120±6	113±22	156±7	172±4	192±3	190±2	215±3	238±4	252±5															
NGC 4845	46±11(0.11)	136±8	184±4	203±3	201±6	161±7	170±11	181±4	181±7	181±1																
NGC 6314	...	...	...	231±2	...	232±6	248±6	245±4	...	...	216±4	233	225±5	...	...	222±3	228±2									
IC 720	...	...	...	...	...	376	347	369±9	346	343	328	...	...	281	274±7	254	290±10	277±3	273±2	276±5	302±3	272±1				
UGC 10205	-28±2(0.10)	...	99	83±29	98	160±17	...	201±6	194	215±9	218±5	217±2	238±2	252±12	272±7	...	...	241	245±8	243±5						
UGC 10205						~20	~23±9	-16±16	2	7±11	92±3	164±7														
UGC 10205								130	52																	
Sb																										
NGC 1085	...	...	...	253±13	270±8	292	295±5	306±3	302±5	304±3	303±8	292±3	297±3	309±2	301±5	300	299±4	285±1	307±10	328(25.5)						
NGC 1325	-15±5(0.06)	54±5	82±7	93±8	107±3	121±3	131±2	134±2	149±1	158±4	163±2	165±2	179±2	184±1												
NGC 1353	11±3(0.04)	180±5	154±4	...	207	...	174	189±3	191±6	234	229±9															
NGC 1617	34±84(0.01)	...	188±18	225±17	248±11	256±8	260±4	266±2	269±2	264±5	261±2	261±5	270±5	256±4	262	273±3	288±5	310±1	...	332±12						
NGC 1515	39±10(0.05)	115±9	196±10	229	...	...	204±1	163±7	172±3	162±3	164±2	149±3	165±3													
NGC 1620	...	77±16	113	98±18	135±9	158±2	180±2	177±3	173±6	181±3	202±3	212±3	212±1	220±2	231±2	226±6	232±3	250±4								
NGC 2599	broad	broad	broad	broad	broad	...	221±27	211±13	207±3	201±2	203±5	220±3	234±4	241±4	252±5	252±8										
NGC 2708	broad	93±5	95±8	103	120±7	...	214	162±3	193±14	225±2	239±4	227±4														
NGC 2815	13±15(0.0)	260	232±21	271	269±3	279±8	297	296	267±7	274±4	271±3	266±2	...	...	...	278±12	278±3									
NGC 3054	...	...	46	82	74±14	132±10	173±25	172	183±11	199±8	...	220±4	230±6	257±5	166±24	241±4	...	233±12								
NGC 3067	17±8(0.13)	56±4	87±2	104±2	119±1	127±1	129±1	138±2	142±1	148±1																
NGC 3185	...	226±2	203±1	...	...	...	...	238±2	218±11	240	251±5	266±4	255±4	249±3	264	258±6	264±2	286±2	...	261±3						
NGC 3200	4±(0.10)	103±64	161±22	219	280	263±1	237±12	221±17	217±10	245±8	253±3	263±5	268±5	261±7	265±6	276±6	270±5	275±3	266	283±6	277±4	...	271±13			
NGC 3223	...	...	45±10	75	...	...	228±6	236±8	243±5	253±4	239±8	236±5	246±7	250±7	269±4	274±13	265±9	280±3	261±11							
NGC 4448	3±1(0.01)	...	...	...	...	163±7	179±2	183±2	190±4	197±1	187±3															
NGC 4480	32±40(0.12)	134±4	146±2	148±2	165±2	173±2	169±5																			
NGC 7083	...	...	...	...	165±15	194±7	194±3	180±16	203±9	191±6	215±5	214±5	214±9	228±8	219±4	214±7	208±7	214±6	225±16	223±6	222±8	217±6				
NGC 7171	26±9(0.01)	12±11	9	...	65	107	173±13	189±9	187±23	213±18	212±1	211±7	216±7	196±7												
NGC 7317	...	...	212±7	254±5	284±5	266±7	268±3	...	265±3	284±4	267±6	241±4														
NGC 7537	8±4(0.10)	30±3	66±8	84±5	108±2	134±2	142±3	139±5	140±4	139±2	138±1	138±1	143±2	141±1	135±2	142										
NGC 7606	-4(0.0)	...	...	...	...	...	189	211±4	225±5	243±3	257±3	270±3	273±1	272±1	273±2	258±3	253±2	262±2	268±2	261±3	280±4					
UGC 11810	1±3(0.0)	...	84±2	104	128±1	116	131±4	146±6	...	161±5	164±4	164±5	173±4	171	173±1	179	173±4	214	188							
UGC 12810	25±79(0.05)	56±38	...	...	...	...	...	...	...	...	...	183	208±3	204±13	206±7	214±2	213±6	218±2	228	218±6	222±4	229±4	229±1	...	238±3	
Sc																										
NGC 791	53±3(0.07)	61±2	51±2	62±1	85±2	89±3	108±3	125±3	141±4	151±3	139															
NGC 753	...	142±5	180	...	153±12	160±3	176±7	195	210±9	209±11	203±4	201±5	204±1	209±6	216±6	223±4	200±3	211±8	210±7							
NGC 801	...	...	...	119±1	137±16	198±2	221±8	230±2	...	211	205±3	212±5	227±8	210±8	213±5	220±2	225	225±2	219±6	191±2	205±4	206±7	202±1	205±7		
NGC 1035	19±1(0.15)	38±2	65±3	80±3	90±3	106±3	121±1	122±2	125±3	133±3																
NGC 1087	-4±8(0.08)	69±17	88±6	98±4	112±3	119±4	118±4	115±3	109±4	118±6	132±2	136±3														
NGC 1421	37±16(0.19)	78±6	100±4	122±7	150±7	175±2	168±4	160±8	145±9	150±8	155±6	158±4	162±4	174±4	178±4	195±4	192									
NGC 2608	1±1(0.01)	108±9	122	...	109±1	...	97	...	109±6	110	100±6	...	132													
NGC 2715	32±13(0.09)	53±3	72±5	88±8	98±3	106±2	116±1	124±2	134±1	139±1	153	140±2	137±2	123±6	137±3	156±2										
NGC 2742	15±7(0.08)	47±5	93±9	107±5	114±5	130±2	136±2	151±3	159±2	159±4	165±2	173±4														
NGC 2998	...	86±10	...	120±4	...	142±2	167±7	193±5	196±2	199±2	182±5	180±2	197±4	212±3	...	188±4	207±5	220±2	...	191	213±5	207±5				
NGC 3495	7±8(0.168)	41±4	57±3	66±2	77±2	90±4	118±2	128±3	135±4	129±3	149±5	167±3	171±4													
NGC 3672	1±2(0.01)	8±6	28±4	...	60±6	120±10	162±17	175±10	166±3	162±4	182±3	165±7	172±3	186±3	187±9	186±15										
NGC 4062	39±6(0.08)	73±6	94±4	105±2	121±3	129±2	142±3	148±2	162±3	162±3	147±5	154±13														
NGC 4321	83±15(0.18)	133±6	137±5	118±4	123±14	163±12	188±12	189±5	188±5	178±7	184±8	207±7	199	213±6												
NGC 4605	11±2(0.13)	37±2	60±1	60±3	76±3	89±3																				
NGC 4682	4±22(0.09)	63±12	90	108±4	122	114±9	141±6	139±10	149±6	160±2	170±4	170±4	176±4	163±6												
NGC 7541	...	165±1	173±1	174	157±2	155±7	152±3	150±3	168±6	168±5	190±6	191±6	211±4	218±5	209±6	220±3	221±11	257±1								
NGC 7552	...	...	137	138	148±5	157±3	157±3	178±3	186±2	188±6	193±3	189±6	183±4	179±1	...	...	...	...	...	203±8						
IC 467	9±9(0.05)	37±5	95±6	77±4	82±4	96±6	106±5	115±6	125±2	127±4	122±2	129±4	162	131±6	125±3	148±2	145±4	145								
NGC 2985	...	...	208	297±42	301	...	...	269±2	260±4	252	257±7	278±7	260	261	249±2	238	290±6	298±7	261	266±7	295±2	309±2	306±7	299±3	309±5	303±63	292±9
NGC 3621	17±(0.06)	24±8	33±7	39±5	55±2	78±5	94±2	91±3	102±4	105	115±12	116±4	133±2	133±3												

Fig. 7

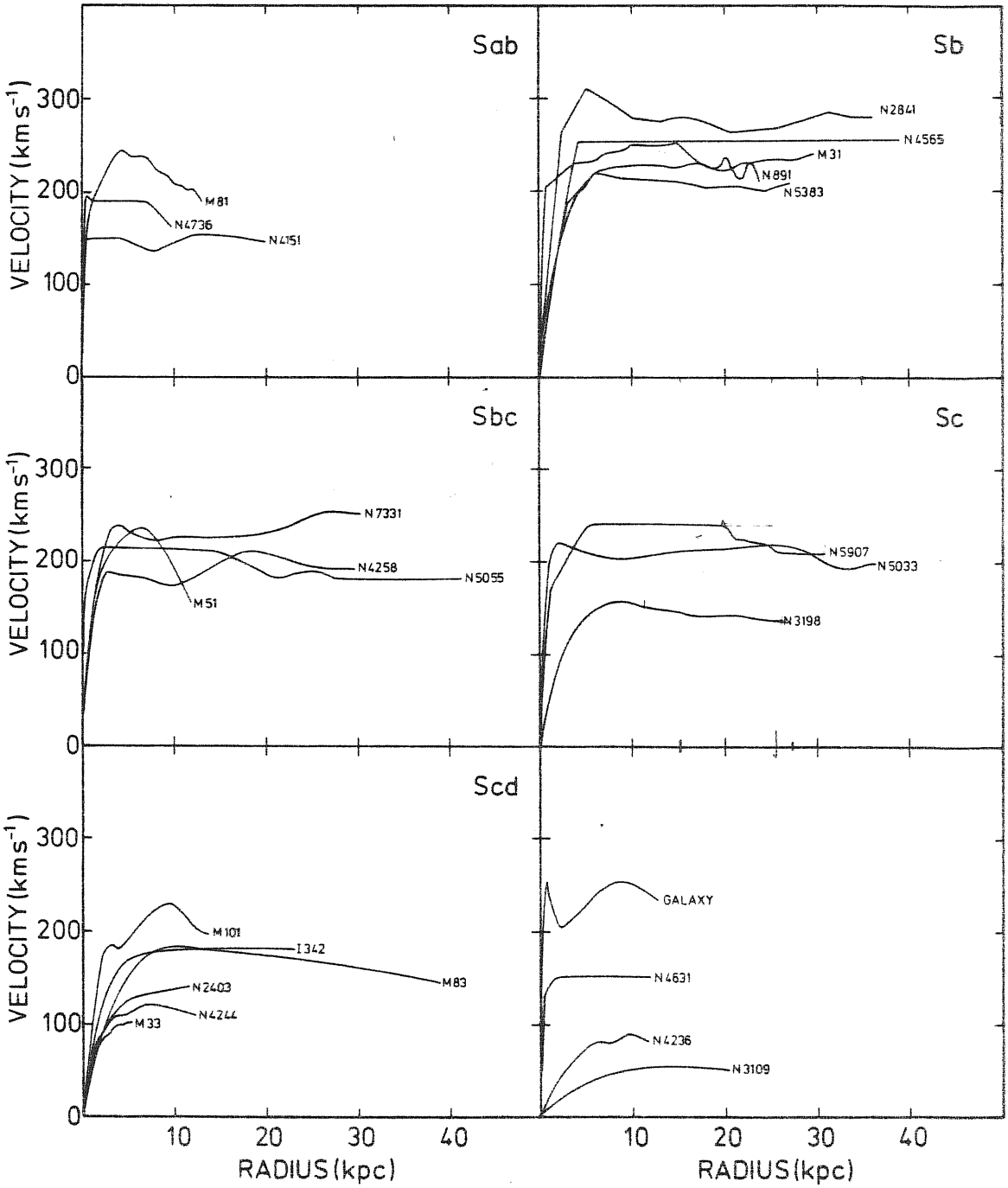
Sab
Sb
Sbc
Sc
Scd
VELOCITY (km s⁻¹)
0
100
200
300
M81
N4736
N4151
N2841
N4565
M31
N891
N5383
N7331
N4258
N5055
M51
N5907
N5033
N3198
M101
I342
M83
N2403
N4244
M33
GALAXY
N4631
N4236
N3109
10
20
30
40
RADIUS (kpc)

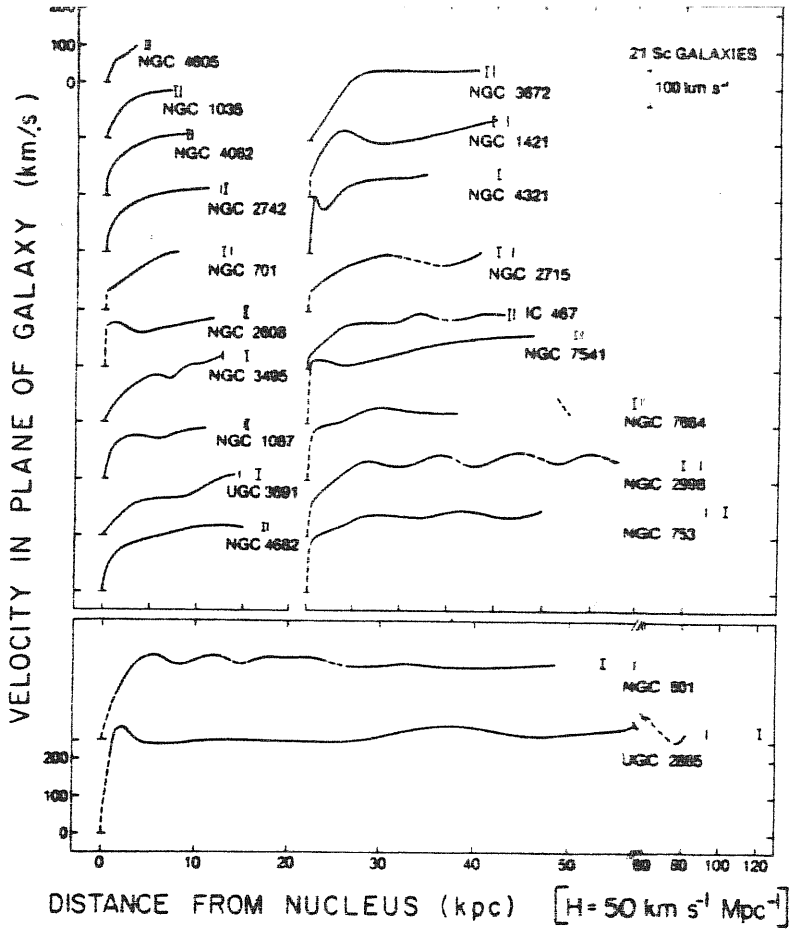

FIG. 5.—Mean velocities in the plane of the galaxy, as a function of linear distance from the nucleus for 21 Sc galaxies, arranged according to increasing linear radius. Curve drawn is rotation curve formed from mean of velocities on both sides of the major axis. Vertical bar marks the location of R_{25}, the isophote of 25 mag arcsec^{-2}; those with upper and lower extensions mark R^{c}, i.e., R_{25} corrected for inclination and galactic extinction. Dashed line from the nucleus indicates regions in which velocities are not available, due to small scale. Dashed lines at larger R indicates a velocity fall faster than Keplerian.

FROM RUBIN

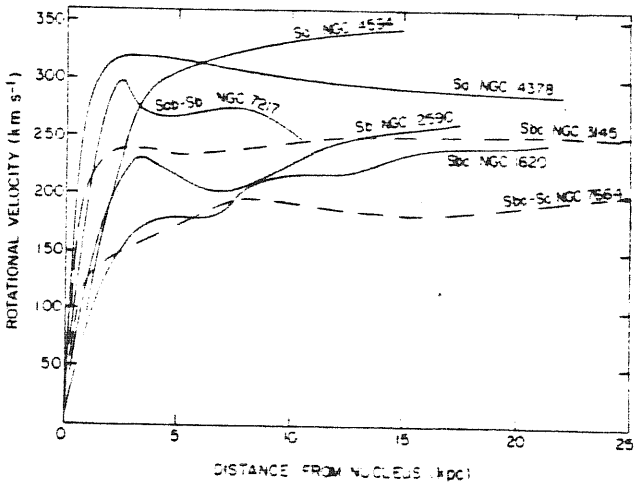

FIG. 3.—Rotational velocities for seven galaxies, as a function of distance from nucleus. Curves have been smoothed to remove velocity undulations across arms and small differences between major-axis velocities on each side of nucleus. Early-type galaxies consistently have higher peak velocities than later types.

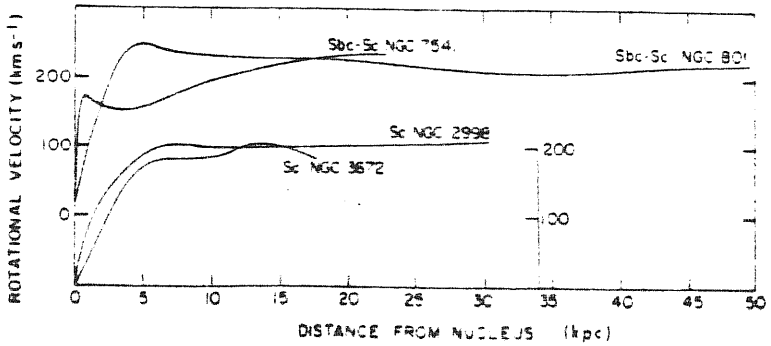

FIG. 4.—Rotation curves for two pairs of galaxies, which illustrate the lack of Tully-Fisher relation. NGC 7541 and NGC 801, both Sbc–Sc, have V_{max} values of 238 and 248 km s^{-1}. However, their luminosities (7.05 ± 0.7 and 23.8 ± 9 × 10^{10} $L_\odot$) and radii (23.2 and 49.1 kpc) differ by factors of 3 and 2. Similarly, the Sc galaxies NGC 2998 and NGC 3672 have V_{max} of 211 and 208 km s^{-1}, but luminosities 14.9 ± 1.4, 4.45 ± 0.4 × 10^{10} $L_\odot$ and radii 34.0 and 17.6 kpc.

tly increasing: an old theorethical picture typically $V(R_f) - V(R_M) =$

$-(50\ 100)$ Km s^{-1} at the contrary from (214)

$$V(R_f) - V(R_M) = +(0 \sim 20) \text{ Km s}^{-1}$$

In Sa, Sb galaxies is present a quite large bulge $\sim 1-6$ Kpc

detected also by dynamics: we find a transition region between bulge and disk how it is aspected by the fact that bulge and disk surface density have a much different dependency on R.

That transition would be aspected where the contribute of halo becomes important, say $R \sim \frac{1}{2} R_{25}$ nevertheless do no track appears in rotation curves.

However the greatest contrast between the exponential disk picture and the observative one is in $\frac{dV}{dR}$ rather than in V itself.

Infacts while $\left.\frac{dV}{dR}\right|_{\text{exp disk}} \sim -20$ Km s^{-1} Kpc^{-1} we have $\left.\frac{dV}{dR}\right|_{\substack{\text{OBS} \\ \text{AXISYM}}} \sim 2$ Km s^{-1} Kpc^{-1}

so that the axisymmetric contribution is remarkably less than the contribution of self gravity of arms, or of any non-circular motion

$$\left.\frac{dV}{dR}\right|_{\substack{\text{NOT} \\ \text{AXISYM}}} \sim 10 \text{ Km s}^{-1} \text{ Kpc}^{-1}$$

Then, at difference from old predictions it is problematic to discriminate the true axisymmetric derivative of the background gravitational field from the non-circular one.

The observational velocities roughly constant whitin each galaxy are found to vary with morphological Hubble Type $V(Sa) > V(Sb) > V(Sc)$ this has a simple explanation: for Sc galaxies there is more angular momentum

for mass unit opposing to inertia $\lambda = \frac{\dot{L}}{M} = \frac{VR}{G^{-1}V^2R} \propto V^{-1}$ with respect to Sa galaxies, there under the same perturbation amplitude the response would be more evident in Sc galaxies that in Sa ones.

We conclude stressing that from this observative picture has not great meaning to fit data with high polinomials or many parameters fits: the axisymmetric gravitational field doesn't seem to have more than one or two degrees of freedom; if we are interested on it we can write

$$V(R) = \Sigma V_n R^n \qquad (2.44)$$

but to agree with observation:

$$n \text{ must be low} \qquad (2.45)$$

and for $n>2$ $\quad \frac{V_n R^n}{V} \ll 1$ for every R.

Note, besides, that the positions of maxima of undulations found in some rotation curves coincide [32] with spiral arms: those ones, therefore, are just dynamical manifestation of self-gravity of spiral arms.

LOCAL STABILITY OF ROTATING DISK

We ask for the condition that would be needed for the galactic disk to remain gravitationally stable against all large scale disturbance from a local analisis point of view. [15]

We recall that infinitesimally thin self gravitating disk couldn't long endure in presence of the slightest disturbance if there are not considered the stabilizing effects of the Coriolis forces and of the pressure resulting from random motion of individual stars.

Let's begin imagining that the disk suffers at radius R a slight contraction over a small region of linear dimensions L.

This local shrinkage has increased the surface density μ by a fraction ε

Then the increment of the distance is $\sim \varepsilon L$ and in the gravitational force is $\sim \varepsilon G\mu$ which would tend to make the affected region collapse.

On the other hand, by angular momentum conservation, the local angular velocity Ω_{local} must have increased by the factor ε , it produces an increment on centrifugal forces per unit mass of the order of $\sim \varepsilon L \Omega^2_{local}$

Then centrifugal forces aren't able to overcome the former imbalance if the perturbation has wavelenght sufficiently shorter than

$$L_c \simeq \frac{G\mu}{\Omega^2_{LOCAL}} \simeq \frac{\mu}{\mu_{MEAN}} \left(\frac{\Omega}{\Omega_{LOCAL}}\right)^2 R \qquad (2.46)$$

$$\simeq R \quad \text{(Typical galactic Radius)}$$

The criterion for the prevention of an earlier instability by the ra
motions is that a typical mass element has an amount of random veloc
so large to travel through the region of dimension L before the dist
bance amplitude would have grown of a factor e ; i.e. we must have, t
stabilize perturbations:

$$L \leq L_j \cdot \langle V_R \rangle / G\mu \qquad (2.47)$$

Where $\langle V_R^2 \rangle$ is the radial dispersion velocity.

We can see that if $L_j = L_c$ all wavelenght are stabilized: the combine
effect of rotation and random pressure would damp any local instabili-
ties; the exact value for $\langle V_R \rangle$ can be worked out studing the effect of
a disturbance on the velocity distribution function $f(V_R, V, R, t)$ by mea
the collisionless Baltzmann equation [15]

$$\frac{\partial f}{\partial t} + V_R \frac{\partial f}{\partial R} + \frac{V^2}{R}\frac{\partial f}{\partial R} - \frac{V_0 V}{R}\frac{\partial f}{\partial V} + F_R \frac{\partial f}{\partial V_R} = 0 \qquad (2.48)$$

where $f = f_0(V, R) + f_1(V, V_R, R, t)$; the index 1 means a small

$F_R(R)$ is radial force, $F_R = F_{0R} + F_{1R}$ with $F_{0R} = \Omega^2 R$

The solution of ( ) imply for vanishing neutral waves the relationship
for the neutral wavenumber K_m

$$\frac{K_m \sigma_R^2}{2\pi G\mu} = 1 - \exp\left[\left(-\sigma_R^2 K_m^2/K^2\right) I_0\left(\sigma_R^2 K_m^2/K\right)\right] \qquad (2.49)$$

Then from (249) neutral disturbances are damped if

$$\sigma_R \geq \sigma_{R\,Min} = (0.2857)^{1/2} \left(\frac{K}{K_m}\right) = 3.36 \frac{G\mu}{K} \qquad (2.50)$$

and because

$$\sigma_\theta^2/\sigma_R^2 = \frac{1}{2}\left[1 + \frac{R}{V}\frac{dV}{dR}\right] \qquad (2.51)$$

$$\sigma_{\theta,Min} = 0.7\ \sigma_{R,Min}$$

Because

$$m \sim 4\pi\mu R^2 \sim G^{-1}V^2R \quad \text{and} \quad K^2 \sim 2\left(\frac{V}{R}\right)^2 \quad \text{we have:}$$

$$\sigma_R/V \simeq \frac{3.36}{} \sim 0.18$$

$$\sigma_\theta/V \sim 0.13$$

Then to avoid local instabilities, matter rotating at radius R with linear velocity V must have both a radial component (20% of the rotational one) and a tangential non rotational component (10%).

We conclude this section with some comments:

galaxies have been found stable against local instabilities i.e. instabilities that would *enhance* the occurrence of strong two body scatterings producing lumps of matter in the disk and expulsion of stars outside the disk, but what about global coherent large scale instabilities? The neutral ones have an important role in the formation and survival of Spiral design (chapter III); more complicated is when global instabilities evolve with time, then is possible only N-Body simulations analysis.

The latter ones give an alternative explanation of the spiral phenomenum: non more a steady pattern but an evolving configuration which for

most part of the time resembles to a global spiral-like Grand Design.

CHAPTER 3

THE SPIRAL PATTERNS

SPIRAL STRUCTURE AS A QUASI STEADY DESIGN

The most impressive feature in disc galaxies is the presence of an impo sing spir-like Global grand Design; for istance see the Galax M 101 .

QSSS picture [5] [12] [13] can be considered, at least far from reso- nances, a good approximation able to explain the principal observative features.

Two are the general hypotesis at the basis of QSSS theory: a) behind the spiral phenomenum there is just Gravitation; b) gravitation acts trough the creation of spiral wave; this wave it is supposed to propaga te radially but it is hoped that it happens in scale time longer that the life of the Universe.

It is important to realize that:

1) the spiral arms are associated with gas (often ionized) and young (massive) stars: in a galaxy the density contrast between the brighter and darker regions is small. [33] see fig (2B)

2) The regularity of the pattern extends over the whole disk [33]

QSSS theory postulates that a nearly neutral spiral wave provides the spiral gravitational field underlying the observable spiral arms.

We notice that transient local pattern of a general spiral form are re- latively easy to produce in a rotating system, [18] nevertheless it is rather difficult to account for a coherent pattern over the whole disk without considering the cooperative effects of long-range gravitational

forces.

Let us begin imponing for the density, velocity, gravitat... per

turbations the spiral form:

$$\begin{aligned} \mu &= \mu_0(R) + \mu_1(R,\theta,t) \\ V_R &= V_{R1}(R,\theta,t) \\ V_\theta &= V_{00}(R) + V_{\theta 1}(R,\theta,t) \\ \phi &= \phi_0(R,z) + \phi_1(R,\theta,t) \end{aligned} \qquad (3.1)$$

where

$$\begin{aligned} \mu_1 &= \\ V_{R1} &= \\ V_{\theta 1} &= \\ \phi_1 &= \end{aligned} \left[\text{Real} \left| \begin{array}{l} \hat{\mu}_1(R) \\ \hat{V}_{R1}(R) \\ \hat{V}_{\theta 1}(R) \\ \hat{\phi}(R) \end{array} \right| \times e^{i(\omega t - m\theta)} \right] \qquad (3.2)$$

The quantities $\hat{\mu}_1, \hat{V}_{R1}, \hat{V}_{\theta 1}, \hat{\phi}_1$ called collectively $\hat{q}$ are in general complexes; we write them as

$$\hat{q} = A(R)\, e^{i\Gamma(R)} \qquad (3.3)$$

and we make the hypotesis of tightly wound spirals:

$$\begin{aligned} &A(R) \text{ varies slowly} \\ &\Gamma(R) = \Lambda_0 f(R) \qquad \Lambda_0 \text{ great parameter} \qquad (3.4) \\ &f(R) \text{ varies slowly} \end{aligned}$$

Infacts the lines of constant (maximum) μ_1 are approximately given by

$$\omega t - m\theta + \Gamma(R) = 2\pi \qquad (3.5)$$

(3.5) represents (for each istant t) a m-armed spiral pattern described by

$$m(\Theta - \Theta_0) = \Gamma(R) - \Gamma(R_0) \qquad (3.7)$$

The pattern rotates with a uniform angular velocity Ω_p

$$\Omega_p = \text{Real}\left\{\frac{\omega}{m}\right\} \qquad (3.8)$$

For showing an exemple we consider the logarithmic spiral

$$\Gamma = \Lambda_0 \ln R \qquad (3.9)$$

The pitch angle defined as

$$i = \text{arctg}\left[m(K_2 R)^{-1}\right] \qquad (3.10)$$

$$K_2 = \frac{d\Gamma}{dR} \qquad (3.11)$$

is $$i = \text{tg}^{-1}\left(m/\Lambda_0\right) \qquad (3.12)$$

the spacing between spiral arms is given by

$$\lambda = \frac{2\pi}{K_2}$$

Trailing pattern means $K_2 < 0$.

Before a dynamical investication, whose outline is in table (3), we stress that supponing a spiral wave pattern, resonances between stars (gas) and spiral wave occur when

$$m(\Omega_p - \Omega) = n K \qquad (3.13)$$

where $n = 0, \pm 1, \pm 2 \ldots$; m is the number of arms and K is the epicycle frequency.

$n = 0$ $\qquad \Omega_p = \Omega$ $\qquad$ COROTATION

TAV. 3

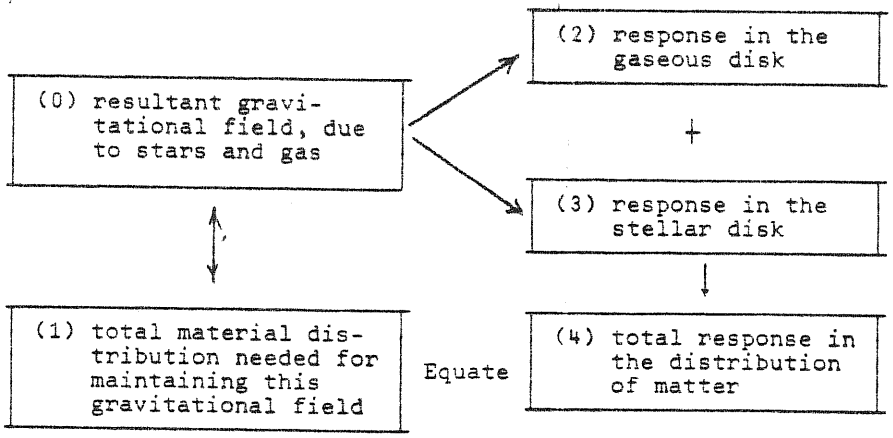

TAV. 4

Observed Features in Spiral Galaxies and their Theoretical Explanation in Terms of Density Waves

Observation	Theory (QSSS hypothesis)
(1) existence of a grand design	(1) wave pattern
(2) persistence of spiral pattern	(2) quasi-stationary spiral structure
(3) spiral pattern usually two-armed	(3) $\Omega-\kappa/2$ nearly constant (Lindblad)
(4) multiple-armed in outer regions	(4) $\Omega-\kappa/m$ nearly constant in outer regions
(5) ring structure (e.g. in NGC 5364)	(5) $\lambda \approx 0$ at resonance
(6) HI distribution follows optical spiral arms[†].	(6) HI concentration at minimum of spiral gravitational potential.
(7) HII regions arranged like a string of beads.	(7) galactic shock triggering star formation
(8) dust lanes on inner side of bright spiral arms.	(8) gas compressed at galactic shock before stars form.
(9) abundance distribution of ionized hydrogen varies greatly over the disk; none inside ring, except at center.	(9) gas compression and rate of star formation vary with radius; wave pattern becomes tightly wound and terminates as resonance is approached.
(10) peak of abundance distribution of neutral hydrogen outside of HII distribution.	(10) shock mechanism needed for star formation ; not available in outer regions.
(11) magnetic field generally weak, but appears to be intensified along the dust lane in certain galaxies (e.g. M51)[†]	(11) absence of perennial stretching by differential rotation; field increased by compression of gas.

[†]Well established by WSRT observations after theoretical predictions had been made.

$n = 1 \qquad \Omega_p = \Omega - K/2 \qquad$ INNER LINDBLAD RESONANCE

$n = -1 \qquad \Omega_p = \Omega + K/2 \qquad$ OUTER LINDBLAD RESONANCE

The esistence of these resonancesis fundamental for QSSS theory: there are no spiral (quasi) modes if resonances are absent [12] (Antispiral theorem).

We study the dynamics writing up the continuity and motion equation and couple them with the Poisson equation.

$$\frac{\partial \mu}{\partial t} + \frac{1}{R}\left\{\frac{\partial}{\partial R}\left(R\mu V_R\right) + \frac{\partial}{\partial \theta}\left|\mu\left(R\Omega + V_\theta\right)\right|\right\} = 0$$

$$\frac{\partial V_R}{\partial t} + V_R \frac{dV_\theta}{dR} + \left(\Omega + \frac{V_\theta}{R}\right)\frac{\partial V_R}{\partial \theta} - \frac{\left(R\Omega + V_\theta\right)^2}{R} = -\frac{\partial \phi}{\partial R} - \frac{a_0}{\mu}\frac{\partial \mu}{\partial R}$$

$$\frac{\partial V_\theta}{\partial t} + V_R \frac{\partial}{\partial R}\left(R\Omega + V_\theta\right) + \left(\Omega + \frac{V_R}{R}\right)\frac{\partial V_\theta}{\partial R} + V_R\left(\Omega + \frac{V_\theta}{R}\right) = -\frac{1}{R}\left(\frac{a_0^2}{\mu}\frac{\partial \mu}{\partial \theta} - \frac{\partial \phi}{\partial \theta}\right) \qquad (3.14)$$

$$\frac{\partial^2 \phi}{\partial R^2} + \frac{1}{R}\frac{\partial \phi}{\partial R} + \frac{1}{R^2}\frac{\partial \phi}{\partial \theta^2} + \frac{\partial \phi}{\partial z^2} = 4\pi \mu_{TOT}\,\delta(z)$$

Note that $V = \Omega R$ defined in (2.1) is different from $V_\bullet$ by a perturbation term following (3.2).

$$V_\bullet = V(R) + V_1(\theta, R, t)$$

a_0 is the turbolent velocity if we take into account also the gas contribution.

In the ground state we have

$$\Omega^2 R = \frac{\partial \phi_0}{\partial R} + \frac{a_0^2}{\mu_0}\frac{\partial \mu_0}{\partial R} \qquad (3.15)$$

then substuting ( ) in (3.4) within the assumption $(K_z R)^{-1} \gg 1$ we get the system

$$\begin{bmatrix} \nu & \left(\frac{K_z}{K}\right)\mu_0 & 0 \\ 0 & i\left(\nu^2-\left(\frac{K_z}{K}\right)^2 a_0^2\right)/\nu & -2\frac{\Omega}{K} \\ 0 & \frac{K}{2\Omega} & i\nu \end{bmatrix} \begin{bmatrix} \hat{\mu} \\ \hat{\cdot} \\ \hat{V} \end{bmatrix} = \begin{bmatrix} 0 \\ \left(\frac{\partial \phi_1}{\partial R}\right)/K \\ 0 \end{bmatrix} \qquad (3.16)$$

where

ν is the frequency at which gas particles encounters a periodical gravitational field.

Then we get the first important result:

$$\frac{\hat{\mu}}{\mu_0} : \frac{\hat{V}_\theta}{V} : \frac{\hat{V}_z}{V} = (-K_z R) : m\left(\frac{\Omega_0}{\Omega}-1\right) : i\frac{K^2}{2\Omega^2} \qquad (3.17)$$

Using Poisson equation we get :

$$\frac{\partial \phi_1}{\partial R} = 2\pi i G \mu \, \mathrm{sgn}(K_z) \qquad (3.18)$$

so

$$\frac{\hat{\mu}}{\mu_0} = \mathrm{sgn}(K_z) \quad \frac{K_z G \hat{\mu}}{K^2(1-\nu^2)+K_z^2 a_0^2} \qquad (3.19)$$

We obtain also the dispersion relation

$$\left(\frac{K_z}{K_T}\right) = (1-\nu^2) + \left(\frac{K_z^2}{K^2}\right) a_0^2 \qquad (3.20)$$

Introducing the wavelenghts

$$\lambda = \left|\frac{2\pi}{K_z}\right| \qquad \lambda_T = \frac{2\pi}{K_T} \qquad (3.21)$$

We rewrite (3.20) in the form

$$X_T = \left(\frac{\lambda}{\lambda_T}\right) - (1-\nu^2)\left(\frac{\lambda}{\lambda_T}\right)^2 \qquad (3.22)$$

where $X_T = K_T a_0^2/K^2$

if turbolence it is assumed to be produced only by instabilities then

$\chi_T = 1/4$ [15] and we get

$$\frac{\lambda}{\lambda_T} = \frac{1}{2}\left[\frac{1}{1 \pm \nu}\right] \qquad (3.23)$$

There are two branches in the solution long and short branch.

We note this is the hydrodynamical approach to the problem valid for the gas component but not for the stellar component, whose is an approximation only far from the resonances; in particular gas pressure blunts the resonant effect.

We would have used the kinematical approach for both gas and component to have a complete phisical description, nevertheless at the begin we preferred to show easily why and where dispersion relation comes out further more the idrodynamical approach has had a revival of interest: Berman and Mark [1,2] unified the kinetic and the hydrodynamical approach finding a set of closed moment equations of hydrodynamic form derived from collisionless Boltzmann equation:

$$\frac{\partial \mu}{\partial t} + \mu \nabla \cdot \vec{V} = 0$$

$$\frac{dv_R}{dt} = \frac{V_\theta^2}{R} - \frac{\partial \phi}{\partial R} - \frac{1}{\mu}\left[\frac{\partial P_{RR}}{\partial R} - \frac{P_{RR} - P_{\theta\theta}}{R} + \frac{1}{R}\frac{\partial P_{R\theta}}{\partial \theta}\right] \qquad (3.24)$$

$$\frac{d(RV_\theta)}{dt} = -\frac{1}{\mu}\left[\mu \frac{\partial \phi}{\partial \theta} + R\frac{\partial P_{R\theta}}{\partial R} + 2P_{R\theta} + \frac{\partial P_{\theta\theta}}{\partial \theta}\right]$$

Where P_{RR}, $P_{R\theta}$, $P_{\theta\theta}$ are stress components determined by closure equations and $\frac{d}{dt} = \frac{\partial}{\partial t} + \vec{V} \cdot \nabla$

$$P_{\theta\theta} = \frac{K^2}{4\Omega^2} P_{RR} \quad , \quad \frac{d}{dt}\left(P_{RR}/\mu K\right) = 0$$

$$P_{R\theta} = -\frac{P_{RR}}{4\Omega}\left[d\ln\left(\frac{R^2K^3}{4\Omega^2}\right)/dt + 2\frac{\partial\Omega}{\partial\theta}\right] \tag{3.25}$$

In these equation it is assumed $\frac{1}{KR} \sim \varepsilon$ and $\frac{\partial\phi}{\partial\theta}/R\frac{\partial\phi}{\partial R} \sim \varepsilon$ small.

Thus to conserve vorticity

$$\frac{d}{dt}\left(\frac{\mu\Omega}{K^2}\right) = 0 \tag{3.26}$$

Then from (3.24) (3.25) (3.26) , that account for the phisics for gas or stellar disk we derive, pratically as we have done before for the (3.14) (3.15) (3.18) system, the dispersion relation valid (in the single wave picture) everywhere:

$$\frac{\lambda}{\lambda_T} = \frac{1 \mp \sqrt{\gamma s^2(1-\gamma)}}{2(1-s^2)} \tag{3.27}$$

where γ is a simple device to accomodate the gas approximation ($\gamma = 1$) or stellar approximation ($\gamma = 3/2$).

We conclude this section recalling the results obtained by Lin- Shu theory.

First we point out that QSSS theory, as we shall see, has mathematical and phisical defects; furthermore a good comparision with observations needs good rotation curves and good photometry, nevertheless QSSS can account for a first explanation about the spiral phenomenum and indicative comparision can be worked out.

Let us stress again that in the confronts between theory and observations available in literature the main problem, in our opinion, is not some

defectiveness of the theory but the fact that have been used rotation curves and structure models incompatible with recent observations. [24] [28] Those results are shown in Table 3 that well describe the self consistency of the spiral wave theory: for many galaxies it is possible to work out the pattern speed the coratation radius, the pitch angle, and the velocity component of basic rotation normal to the spiral arms which strongly influences the strenght of the galactic shock wave formed in the gas disk

In addition spiral wave can account for individual orbit of young stars fig. (8) and very roughly for some phenomenology listed in table (4)

We present table (3) because it is the beliving at autors of QSSS theory, nevertheless we have strong skepticism about point (3) (4) (5): recent observation [11] don't support them.

We think that would be worthwile to reconsider completely the problem: i.e. to work out some table like table (5) but by using recent theoretical idea on structure of galaxies.

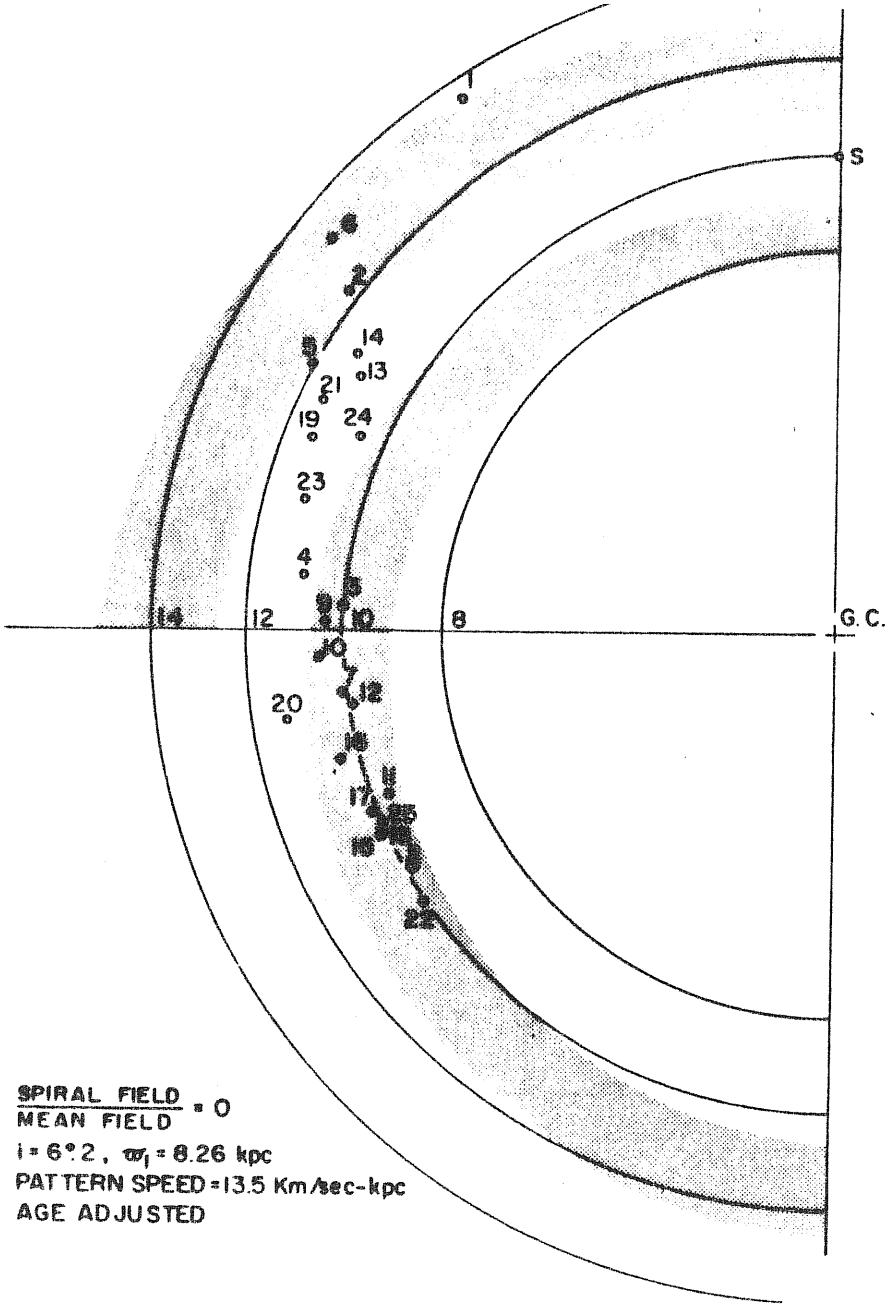

Places of formation of stars as determined without a spiral field.

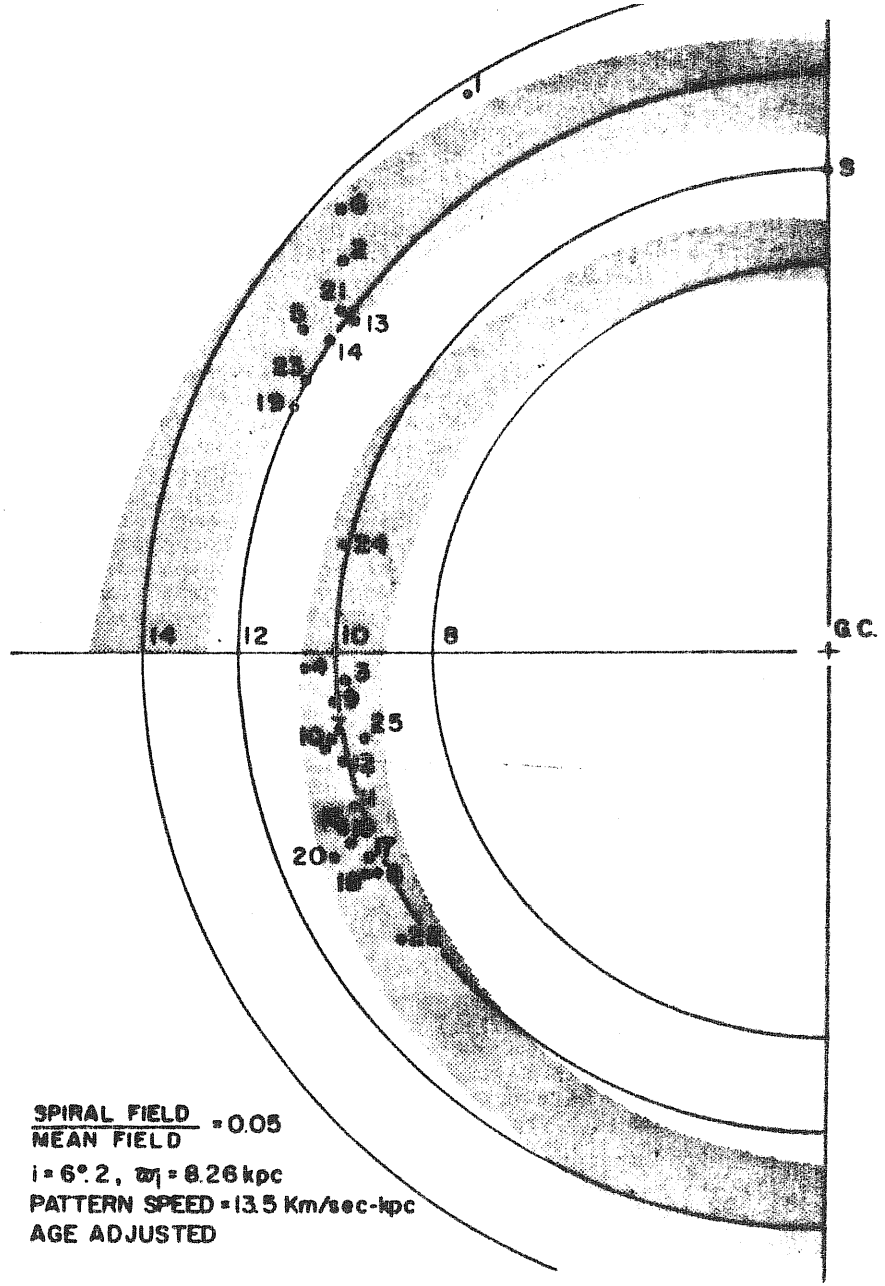

Places of formation of stars as determined with the inclusion of a spiral gravitational field travelling at a pattern speed of 13.5 km/sec-kpc. and having an intensity equal to 5% of that of the Symmetrical gravitational field.

TAV 3

NGC (1)	Type (de Vaucouleurs) (4)	Distance (Mpc) (5)	Inclination (degrees) (6)	Radius of Easily Visible Disk (kpc) (7)	Radius of Outermost H II Region (kpc) (8)	Holmberg Radius (kpc) (9)
157	SAB(rs)bc	24.0	58.6	9.0	8.9	20.2
224	SA(s)b	0.69	77.0	13.0	22.5	19.8
598	SA(s)cd	0.72	55.0	4.8	5.2	8.7
925	SAB(s)d	6.8	53.0	7.7	9.0	13.8
972	I0	22.1	66.3	4.7	4.0	(15.4)
1084	SA(s)c	19.2	65.0	5.2	5.2	(12.9)
1832	SB(r)bc	25.3	60.0	6.0	6.1	(16.2)
2403	SAB(s)cd	3.25	60.0	4.6	6.7	13.7
2903	SAB(rs)bc	7.9	70.0	12.6	5.3	16.1
3031	SA(s)ab	3.2	55.0	8.9	16.2	16.3
3109	Im sp	2.2	90.0	6.0	3.1	(5.9)
3389	SA(s)c	15.0	62.0	3.2	2.6	(8.7)
3521	SAB(rs)bc	8.5	65.5	6.2	7.3	16.8
3593	SA(s)0/a:	7.0	75.0	1.2	4.1	(7.0)
4236	SB(s)dm	3.25	75.0	9.6	...	12.3
4631	SB(s)dsp	4.4	85.0	7.3	7.0	12.2
5005	SAB(rs)bc	14.4	66.0	8.0	5.7	16.8
5055	SA(rs)bc	7.3	58.6	6.5	7.3	17.0
5194	SA(s)bcp	4.0	35.0	5.0	5.5	8.3
5457	SAB(rs)cd	6.9	22.0	15.5	15.3	28.1
6946	SAB(rs)cd	10.1	30.0	12.3	11.9	(27.9)
7331	SA(s)bc	14.4	69.1	18.4	(10.4)	28.5
7479	SB(s)c	35.2	44.5	15.6	(11.6)	(31.3)
IC342	SAB(rs)cd	4.5	25.0	11.0	...	(26.1)

NGC (1)	Mass M ($\times 10^{10}\ M_\odot$) (5)	Half-Mass Radius $\varpi_{0.6M}$ (kpc) (6)	Pattern Speed Ω_p (km s^{-1} kpc^{-1}) (7)	Corotation Radius ϖ_c (kpc) (8)	Central Mass Concentration $\varpi_{0.6M}/\varpi_c$ (9)	Velocity $(\Omega-\Omega_p)\varpi$ (km s^{-1}) (10)	Pitc Angl (0.5ϖ (degre (11)
157	6.8	5.2	22.0	9.0	0.58	78.1	12.
224	17.8	7.0	18.0	14.0	0.50	129.7	9.
598	1.3	3.5	32.0	2.8	1.24	24.8	19.
	(1.9)	(4.7)	(32.0)	(2.8)	(1.67)	(31.3)	(16.
925	1.8	4.9	14.0	7.7	0.64	35.1	14.4
972	1.0	1.8	29.0	4.0	0.46	67.1	8.8
1084	1.9	2.4	27.0	5.2	0.45	80.6	8.6
1832	4.1	3.2	31.0	6.0	0.53	86.4	10.5
2403	2.3	4.5	25.0	4.8	0.93	26.8	19.9
	(3.5)	(6.1)	(24.0)	(4.8)	(1.26)	(36.2)	(17.4
2903	4.3	2.7	38.0	5.4	0.51	101.9	10.2
3031	12.5	5.5	26.0	9.7	0.57	103.1	11.8
3109	0.5	6.3	8.0	6.0	1.04	6.2	26.1
3389	2.2	2.3	65.0	2.6	0.87	31.6	20.8
3521	8.1	3.2	33.0	7.3	0.44	137.3	8.4
3593	0.2	0.4	80.0	1.2	0.37	73.7	5.4
4236	1.7	6.9	9.0	9.6	0.72	25.1	16.0
4631	2.5	6.2	15.0	7.3	0.84	23.1	19.9
5005	7.3	2.4	27.0	8.0	0.31	180.8	3.9
5055	5.8	2.1	32.0	6.6	0.31	177.6	4.0
5194*	3.3	2.6	42.0	4.5	0.58	77.7	11.7
	[2.4]	[1.2]	[90.0]	[2.4]	[0.51]	[106.9]	[9.6
5457	14.5	10.9	13.0	15.5	0.70	58.9	15.7
	(19.4)	(13.5)	(13.0)	(15.5)	(0.87)	(58.0)	(16.8
6946	11.5	8.1	17.0	12.3	0.66	68.4	14.2
	(19.7)	(12.0)	(16.0)	(12.3)	(0.98)	(74.8)	(14.2
7331	7.8	3.4	19.0	10.4	0.32	152.3	4.9
7479	10.5	9.0	12.0	15.6	0.58	73.3	12.4
IC342	8.8	7.0	15.0	12.5	0.56	78.5	11.6
	(16.0)	(11.3)	(15.0)	(12.5)	(0.90)	(71.3)	(13.8
Our Galaxy.	13.1	6.0	13.5	15.7	0.38	148.1	6.9

TRANSFER OF ANGULAR MAMENTUM TRHOUGH SPIRAL PERTURBATIONS

Trailing spiral structures have an important property: they are able to transfer outwards angular momentum; this transfer involves both the problem of the pattern survival and the angular momentum distribution.

Wa ask: why galaxies want to transfer angular momentum? The answer is simple: if angular momentum flows outwards it lows the level of minimum energy. [6]

To show it, let us study the motion of two particles in a axisymmetric galaxy-like potential $\phi(R,z)$.

Let $m_1, m_2, j_1, j_2, \varepsilon_1, \varepsilon_2$ mass, specific angular momentum, specific energy of two particles.

Fixed j, the minimum value of $\varepsilon = \frac{1}{2}(v_R^2 + v_z^2 + j^2/R^2) - \phi(R,z)$ will occur in the circular orbit of radius R_j for which

$$j^2 R_j^{-3} + \frac{\partial \phi}{\partial R}\Big|_{R_j} = 0 \qquad (3.28)$$

Therefore the minimum specific energy for individual orbit is

$$\varepsilon(j) = \frac{1}{2} j^2 R_j^{-2} - \phi(R_j, 0) \qquad (3.29)$$

with

$$\frac{d\varepsilon(j)}{\partial j} = \Omega(R_j) \qquad (3.30)$$

We minimize

$$E = m_1 \varepsilon(j_1) + m_2 \varepsilon(j_2) \qquad (3.31)$$

subject to the constraint

$$m_1 j_1 + m_2 j_2 = H \qquad (3.32)$$

From (3.32) (3.31) we get

$$dE = m_1 dj_1 (\Omega_1 - \Omega_2) \tag{3.33}$$

because $\frac{d\Omega}{dR} < 0$, if dj_1 is negative(outflow) dE is negative.

To achieve lower energy states a galaxy must find a mechanism of transferring angular momentum outwards.

Axisymmetric perturbations are unable to make it, they produce no gravitational couple between different parts of galaxy.

The stress tensor of gravitation field is

$$T = \left[\vec{a} \otimes \vec{a} - \frac{a^2}{2} \vec{e} \otimes \vec{e}\right] (4\pi G^{-1}) \tag{3.34}$$

where $\vec{e}$ basis field and $\vec{a} \equiv \nabla \phi$

The gravitational torque couple is:

$$\vec{C} = \int \langle \vec{R} \wedge T , \partial S \rangle \tag{3.35}$$

Because

$$\langle \vec{R} \wedge \vec{e}_i \otimes \vec{e}_j \rangle = \vec{R} \wedge \partial S = 0$$

the isotropic part does not contribute to angular momentum transfer.

Thus

$$C_R = C_\theta = 0 \qquad C_z = (4\pi G)^{-1} \int R \tilde{a}_\theta \tilde{\theta}_R \, d \tag{3.36}$$

Notice $\tilde{a}_\theta , \tilde{a}_R$ are non axially symmetric part of $\vec{a}$

Suppose

$$\phi = \underset{\text{AXIALLY SYMM}}{\phi_0} + \underset{\text{NON-AXI SYMM}}{\phi_1} \tag{3.37}$$

$$\phi_1 = S(R) \cos m [\theta - \Gamma(R)] \exp[-K.z]$$

then

$$a_\theta = -m S R^{-1} \sin m(\theta - \Gamma) \exp[-Kz]$$
$$a_R = \left[\frac{dS}{dR} \cos m(\theta - \Gamma) + m S \frac{d\Gamma}{dR} \sin m(\theta - \Gamma)\right] e^{-Kz} \tag{3.38}$$

let $K_2 = -m\, d\Gamma/dR$

Hence

$$C_2 = -\frac{1}{4} m \left(\frac{K_2}{K}\right) \qquad (3.39)$$

Notice $K_2 \simeq K$ for tightly wrapped waves and only trailing spiral have K_2 positive so that transfer angular momentum outwards.

Now let us compute the amount of angular momentum exchangel by the star wave interaction. [6]

We have

$$\Omega_1^{-1} = \frac{1}{2\pi} \oint [\dot{R}]^{-1} dR \qquad W_1 = \Omega_1 \int_0^R [\dot{R}]^{-1} dR$$

$$J_1 = (2\pi)^{-1} \oint [\dot{R}]\, dR = \frac{E - E(j)}{K} = \frac{1}{2} K a^2 \qquad (3.40)$$

$$J_2 = j$$

$$W_2 = \Theta - \left(\frac{2\pi}{K}\right)\left(\frac{a}{R}\right) \cos W_1$$

Where W_1, W_2 are the radial and tangential angle variable; J_1 and J_2 their coniugate momenta.

Taking in account in the axisymmetric Hamiltonian the Spiral perturbative potential ϕ_1 expanded in a Fourier series of angle variables W_1, W_2 is

$$\phi_1 = (4\pi)^{-2} \sum_{e,m} \psi_{em}(J_i) \exp[i(eW_1 + mW_2 + \omega t] \qquad (3.41)$$

The angular momentum exchange between stars and wave is

$$\dot{H} = \Sigma\, \dot{H}_{em}$$

$$\dot{H}_{em} = (8\pi)^{-1} \int_0^\infty \int_0^\infty m \left(e \frac{\partial F}{\partial J_1} + m \frac{\partial F}{\partial J_2}\right) |\psi_{em}|^2 \delta(e\Omega_1 + m\Omega_2 + \omega)\, dJ_1 dJ_2 \qquad (3.42)$$

Where F is the distribution function for star.

We can see from (343) that absorbtion or emission of angular momentum can occur only out resonances:

$$\Omega \pm \kappa/2 = \Omega_p = \frac{\omega}{m} \qquad \ell = \pm 1$$

$$\Omega = \omega/m \qquad \ell = 0 \qquad (3.43)$$

because $\frac{\partial F}{\partial J_1} >> \frac{\partial F}{\partial J_2}$, ILR is an emitter while corotation and OLR are adsorbing resonances.

Of course this exchange will lead to lower energy states only for trailing pattern.

GROUP VELOCITY OF SPIRAL WAVES

The Lin-Shu theory descibes spiral patterns in terms of spiral waves composing with observations. Such a suggestion seems quite attractive ; we stress these waves are not permanent selfconsistent modes of oscillation: spiral wave pattern evolves with time. [16]

A tightly wound spiral wave with frequency ω has a group velocity describing how various information from the disturbance propagates radially.

Let the perturbation surface density be

$$\mu_1 = S(R,t) \cos[\Gamma(R,t) - m\theta] \qquad (3.44)$$

then

$$\omega(R,t) = \partial\Gamma/\partial t \qquad (3.45)$$

and the radial wave number

$$K_2(R,t) = -d\Gamma/dR \qquad (3.46)$$

Substituing (3.44) (3.45) in the dynamical equations (26) (27) as seen in chapter III for wound arms $KR \gg 1$ we get an (approximate) dispersion relation of the kind

$$F(K_2, \omega, R) = 0 \qquad (3.47)$$

the (3.47) can be solved to give

$$\omega = f(K_2, R) = 0 \qquad (3.48)$$

or

$$\frac{d\Gamma}{dt} = f\left(-\frac{\partial\Gamma}{\partial R}, R\right) \qquad (3.49)$$

where partial derivatives themselves vary with time.

Using (3.45) (3.46) differentianting with respect to time and to R we g

$$\frac{\partial \omega}{\partial t} + \left(\frac{\partial t}{\partial K_2}\right)_R \frac{\partial \omega}{\partial R} = 0$$

$$\frac{\partial K_2}{\partial t} = -\left(\frac{\partial t}{\partial K_2}\right) \frac{\partial K_2}{\partial t} \qquad (3.50)$$

The convective derivatives indicate that the frequency and the wavenumber information in a evolving spiral perturbation propagates radially with the speed

$$c_g(R,t) = \frac{dR}{dt} = \left(\frac{\partial t}{\partial K}\right)_R \qquad (3.51)$$

To compute c_g we start from the Lin-Shu dispersion relation

$$[\omega - m\Omega]^2 = K^2 - 2\pi G\mu |K_2| I_\nu(x)$$

$$\nu = (\omega - m\Omega)/K \qquad (3.52)$$

$$I_\nu(x) = \left(\frac{2}{x}\right)(1-\nu^2)\, e^{-x} \sum_{m=1}^{\infty} \left[1 - \left(\frac{\nu}{m}\right)^2\right]^{-1} I_m(x)$$

I is a modified Bessel function and $x = K_2^2 \sigma_{22}^2 / K^2$ involves the radial velocity dispersion of the star necessary to avoid local instabilities (if $Q = 1$)

Defining a dimensionless radial wavenumber ζ

$$\zeta = K_2 / K_T \qquad (3.53)$$

and because

$$\sigma_{22} = (0.2857)^{1/2} \left(\frac{K}{K_T}\right) Q \qquad (3.54)$$

We can write (3.48) (3.52) in the form

$$|v| = N(|\Omega|)$$
$$\omega = m\Omega + \mathrm{sgn}(v)\, K\, N(|\Omega|, Q) \qquad (3.55)$$

then we get [16]

$$\frac{dr}{dt} = c_g = \mp \mathrm{sgn}(\Omega v)\left(\frac{K}{K_T}\right)\frac{\partial N}{\partial |\Omega|} \qquad (3.56)$$

$$\frac{\partial N}{\partial |\Omega|} = (1 \pm 2\,\partial \ln \xi_v(x)/\partial \ln x)\Big/ \frac{2}{\partial |v|}\left(\frac{1-v^2}{\xi_v}\right)$$

We estimate the group velocity for the Galaxy near the Sun: [16]

$$c_g \simeq 10\ \mathrm{Km\ s^{-1}}$$

the minus signs means that spiral waves are already wound so tightly that their information propagates radially inward, away from corotation. Thus spiral pattern as a whole can't survive more than 10 years unless spiral waves were somehow replenished, or it has been proved they are true mode constrained to oscillate back and forth between ILR and corotation.

This important result (TOOMRE 1969) deserves some comments

1) As we shall see Lin-Shu dispersion relation is valid only far from resonance [7], there the single wave picture is meaningless and we must to work out a "quantistic" dispersion relation: the interaction of the wave with a resonance is described as the interaction of a particle with a potential barrier. [8] [9]

Nevertheless, regardless what happens within the resonance region

destructive effects of differential rotation on spiral wave still remains.

Infact because $\frac{d\Omega}{dR}<0$ trailing waves tend to wrap yet more tightly, simultaneusly such packet of waves drift in radius to corresponding LINDBLAD resonance.

2) The value of group velocity depends on the shape and value of rotational velocity; in addition, we stress that both the location of resonances and angular speed of pattern strongly depend on the analysis of rotational velocity data.

We ask: how fast is the destruction of the Grand Design. Toomre answer's $10^9 y$ is biased by two prejudices: a) rotational curves are supposed to follow the exponential disk model; b) in the $\left(\frac{dV}{dR}\right)$ has been taken into account both the axisymmetric contribute and the perturbative one.

Then, an objective of my PHD project is to compute for all the galaxies, whose we have both rotation data and spiral pattern parameters the quantity τ describing the time scale of the evolution of Grand Design

$$\tau = \int_{R}^{R_i} \frac{dR}{c_g(R)} \qquad (3.57)$$

The importance of knowing τ as better as we can is that if we find for a galaxy the value $\simeq 10\ y$, the necessity to supply the spiral wave with energy is very less urgent with respect to the value $\simeq 10^8 y$; it strongly constraints the proposed mechanismas to make the Grand Design survive.

EFFECTS OF RESONANCES AND SPIRAL MODES

At the corotation region, for $Q=1$ the long ch is very close to the short wave branch see [13], its amplitude becomes infinite; such a problems come out also at others resonances.

There, the concept itself of single wave picture is meaningless [8] , so the dispersion relation is largely affected. The physical explanation for it is that we can't neglect the fact that because of the finite (non zero) radial epicycle excursions of resonant stars, each resonance influences a region of the order $\sim 2KR$ (~ 3 Kpc) for our galaxy). That causes interactions between star and wave changing the dispersion relation, so that it leads to finite wavenumber at resonances[8].

By this interactions spiral density waves are amplified in the neighborood of corotation; as the incident wave approaches the corotation it couples to and causes emission of two waves; waveangular momentum is conserved but the wave amplitude is increased by [8][9]

$$A = [A_f^{1/2} + A_R^{1/2}]$$

where A_f is the amplitude of forward-omitted wave relative to the incident signal

$$A_f = e^{\beta} \qquad (3.58)$$

Where

$$\beta = \frac{V'}{V_R}\left(\frac{K}{2\Omega}\right)^2 \left|\frac{d\ln\Omega}{d\ln R}\right|^{-1}\left\{(1-Q) + \frac{\mu_{GAS}}{\mu_{STAR}}\right\}$$

Conseguently we have an increase of angular momentum efflux

which reinforces the spiral structure.

Thus the short trailing wave propagating towards the galactic center can be reflected back by the hot bulge as a long wave: this cause a loop between R_i and R_c .

By macthing conditions of proper phase and amplitude we obtain, as quantum condition, [9] the discrete value of pattern frequency Ω_p and the growth rate γ .

This way the structure doesn't propagate radially but its strongness grows with time till stationarety.

This picture leads discrete unstable spiral modes reaching observable amplitude in a time of the order of $\sim 10^9$ y.

The quantum condition is written as

$$\oint K_2 dr = (2m+1)\pi \qquad (3.59)$$

$$e^{\gamma\tau} = \sqrt{2}$$

where $\tau = \oint \frac{dR}{|\partial\omega/\partial\kappa|}$

For the fastest mode contours of constant perturbation density and its amplitude with location of resonance are shown in fig. with the (old kind) rotation curves assumed.

The apparency of spiral density contour seems to be dominated by the short wave branch of the Lin-Shu-Theory, that therefore can approximate, at lower order, also more complicate spiral modes theory.

We want stress that, while the realization of the importance of phisical processes at corotation is a general result valid in any theory accounting for spiral structure, the discrete modes theories need to be relevant for the problem, that their assumption match with observations. They are

A) Existence of ILR out the bulge.

B) The spirdl structure is a global one.

Without ~~A~~, B, these theories are irrelevants. For A, the answer depends, as we stressed, on rotation curves: R_i is obtained through the implicit equation

$$\Omega_p = \Omega - K/2 \Big|_{R_i} \qquad (3.60)$$

Supposing to know from fotometry the spacing between arms, the value of R_i depends so strongly both on V and on $\frac{dV}{dR}$ (through K), that we think that until now we have very few correct exemples of such a computation.

GLOBAL INSTABILITIES

Even if we believe in theoretical progress about spiral structure and internal dynamics of disc galaxies, we briefly examine the N-Body experiments of Global instabilities of star disks, because they can teach us important gross scale behaviours of disc galaxies.

Many authors have amounted to brute-force time integrations of the highly nonlinear equation of motion of 10^5 gravitationally interacting particles. [17] [26] [27] [3] [4]

The result of these experiments are: fig. (9)

1) Disks with random motions barely sufficient to avoid local Jeans instabilities $V_R = V_{R,Min}$ tend to be grossly unstable for $m=2$ mode (bar).

2) Honesteusly, just a little in them looks like spiral structure and there is nothing of long lived structure.

3) Disks converts themselves in hotter configurations (larger V_R) and tend often to develop oval distortions.

The tendency of bar-making can be avoided if the model follow the empirical rule

$$t \equiv \frac{T}{W} \equiv \frac{\text{ORGANIZED KINETICAL ENERGY}}{\text{POTENTIAL ENERGY}} \lesssim 0.14$$

It easy to show that for locally stable disks $t \simeq 0.14$, unless to embede them in a rigid massim dark halo.

We note, that observations of flat rotation curves constrain to consi-

FIG 9

J. A. Sellwood: Bar Instability and Rotation Curves

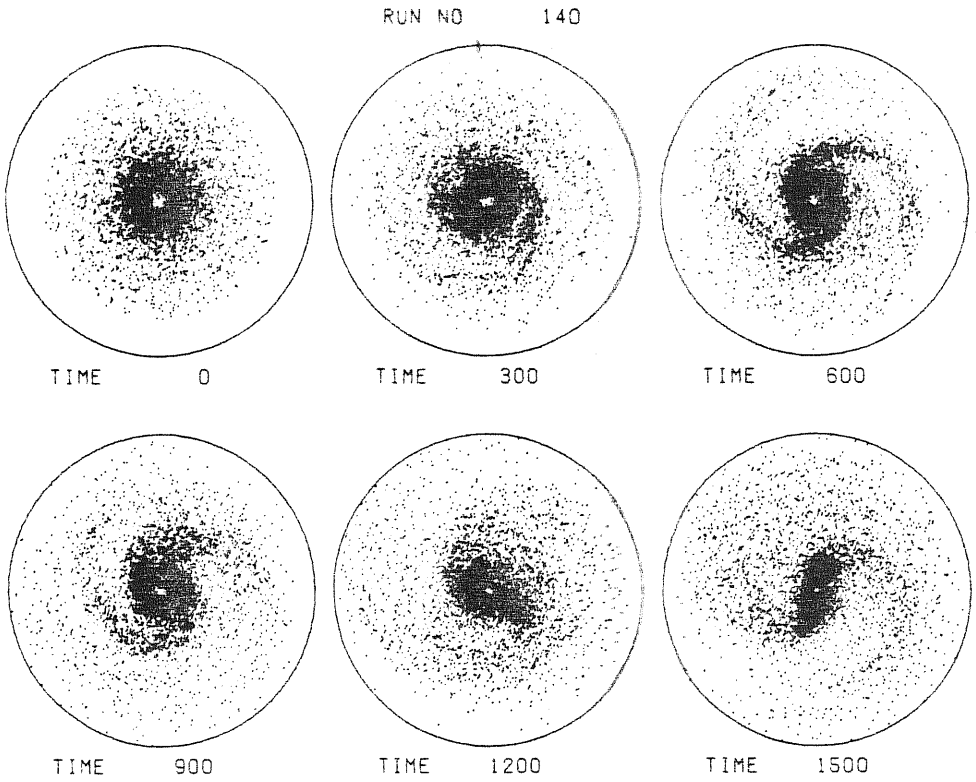

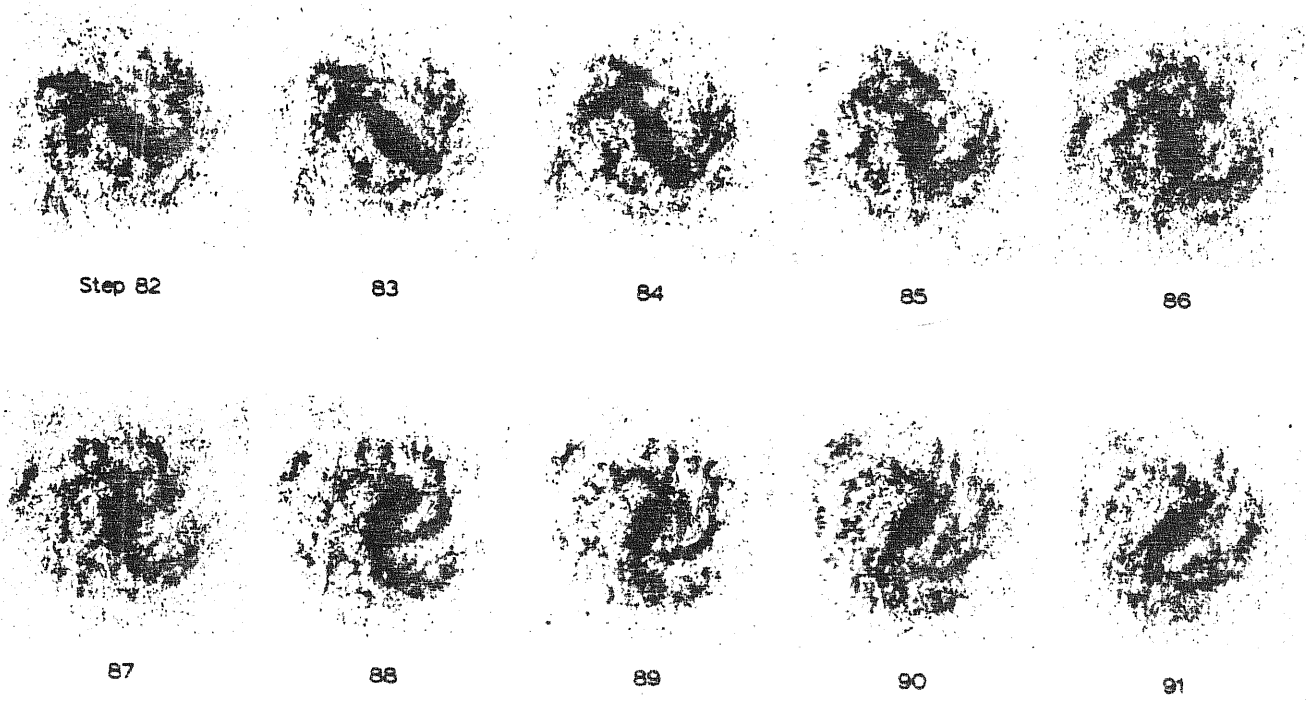

Evolving patterns in the "gas" component of a rotating disk consisting of some 10^5 collisionless "stars." Shown here are the contents of only the central half-squares from Figures 3 and 4 of Miller, Prendergast & Quirk (1970). During this short sequence, the total mass of "gas" decreased from 16.4 to 16.0 per cent of the whole, owing to gradual conversion of such material into additional "stars."

der only disk + halo 3D N-Body experiments.

Great efforts of many authors have been briefly described because we think, despite destruptive criticisms to this approach (for exemple [22]), that it is important to know how gravitation under certain condition, behaves, though we recognise that spiral patterns in galaxies are quite too regular in order that exclude their random formation.

CHAPTER 3

PRELIMINAR RESULTS

In this section we present some preliminar results, as first step, to prove that the idea of an interaction between halo and galactic disk seems to be working to explain the structure and dynamics of spiral galaxies. [33]

It is important to note two crucial points:

1) Despite the general believing [22] that $\Omega - \kappa/2$ $\sim$ constant and it plays an important dynamical role, we have that, because $V \sim$ constant, $\Omega - \kappa/2$ must scale as R^{-1}; then it varies over the whole disk of a factor two.

2) Because $V \sim$ constant its derivative is an order of magnitude smaller that older models predictions.

So we have to take care, analisying data, of discriminating the true background contribute in the derivative from the nonaxisymmetric one.

Introduction

In studying the backgrond axisymmetric and spiral structure it would be worthwhile to find a quantity which keeps constant whithin each object, so that it can be related in an unique way to the other relevant quantities and at the same time its value can help in describing the morphological and dynamical stage of the galaxy.

The aim of this work is to show that $\tilde{V} = (\Omega - \kappa/2) R$ is the above-mentinated quantity and to investigate the consequences of such a result.

The costancy of $\mathcal{V}$

Even in the smoothed rotations curves available in the literature small $< 10\%$ perturbations are present due to the spiral gravitational potential or to other peculiar non circular motions. Though small in value these perturbations -unrelated to the axisymmetric potential- may largely affect the derivative of the velocity field.

We therefore decided to separate the true rotational velocity from the non-circular -and probabily in large part periodical - velocity by fitting the rotational curves given by Rubin et al. [11] [31] from outside the bulge outwards with a linear least-squares fit.

The smallness of those perturbations became apparent from the high values of the correlation coefficients r obtained for the galaxies we have studied (it is aspected that an increase of the amplitude of the non-circular velocity would enhance the scatter of the data points around the theoretical circular velocity).

Since it is $K^2 = 4\Omega^2 \left[1 + \frac{1}{2} \frac{\partial \ln \Omega}{\partial \ln R}\right]$

TABLE 4: NGC NUMBER, BLUE MAGNITUTE, BEST FIT (LINEAR), $\bar{v}$, CORRELATION PARAMETER, $V(R_H)/\bar{v}$, R_H, PERCENTAGE OF (OBSERVATIONAL) ERROR IN ROTATIONAL VELOCITY.

NGC	M_B		V	$\bar{v}$	r	$\frac{V_{RC}}{\bar{v}}$	R_H	$\frac{\Delta V}{V}$
Sb								
3054	-21.63	X	126.8 - 77.4 φ	51.71	0.77	1.62	25.7	0.00
800	-19.55	A	131.1 + 60.2 φ	36.19	0.95	1.95	4.9	001
7537	-21.11	A	115.3 + 51.1 φ	31.88	0.69	1.52	18.3	001
1217	-21.4	A	277.8 - 99.3 φ	83.37	0.95	1.05	15.1	002
15.5	-20.72	X	197.5 - 57.3 φ	50.2	0.91	2.42	13.6	002
1815	-22.04	B	265.9 + 17.5 φ	76.91	0.83	3.64	26.5	00:
7606	-22.67	A	296.5 - 68.5 φ	91.17	0.9	2.7	39.8	0.01
3200	-22.87	A	251.4 + 36.3 φ	71.81	0.96	3.52	46	002
012910	-22.6		203.6 + 30 φ	65.08	0.88	3.61	51.8	001
3145	-22.58	B	233.1 + 52.3 φ	65.87	0.85	4.17	33.8	001
1620	-21.5	A	161.2 + 117.8 φ	43.31	0.57	5.73	28.8	002
1085	-22.4	A	305 ( )	89.33		3.17	34.8	0.01
00810	-21.2		242.6 + 12.2 φ	42.26	0.88	4.66	34	0.01
7171	-21.39	B	192.9 + 40.7 φ	54.61	0.79	3.9	23.9	003
4448	-20.4	B	136 + 104 φ	36.83	0.84	5.16	11	0.01
1325	-20.87	A	112.9 + 88.8 φ	30.41		6.05	18.8	0.01
3223	-22.44	A	236.6 + 28.3 φ	67.82	0.89	3.76	34.8	003
7083	-22.37	A	207.4 + 18.5 φ	65.02	0.69	3.41	39	001
2708	-18.8	A	136 + 157.3 φ	36.2	0.95	6.15	14.7	001
2530	-21.9		153.8 + 211.4 φ	42.34	0.88	6.05	39.6	0.01
1417	-22.28	X	237 + 70.3 φ	66.44	0.76	4.17	33.7	0.01

Sc	NGC IC	LH_β	ΔM	V	$\bar{v}$	$\frac{V_{RC}}{\bar{v}}$	r	R_{25}	$\frac{\Delta V}{V}$
	2998	X -22.38	-0.55	184.9 + 43.6 φ	52.41	4.1	0.88	40	.02
*	801	-23		226 - 23.2 φ	67.88	3.41	0.69	53.5	.02
	3495	? -20.88		88.4 + 103.5 φ	23.53	7.6	0.33	15.2	.02
	3421	X -21.95	-0.82	105.3 + 100 φ	28.27	7.36	0.33	19.5	.02
	2608	B -20.73		71 + 78.8 φ	18.95	7	1	15.1	.05
	2742	P -20.45		114.7 + 73.6 φ	31.77	5.51	0.96	12.5	.02
	4062	-18.6	+1.4	96.9 + 77.9 φ	26.19	6.2	0.94	8.8	.04
	1035	A -19.7	0.94	80.3 + 57.4 φ	21.8	5.9	0.82	7.46	.02
	3672	A -21.15		174.1 + 21.2 φ	49.86	3.85	0.86	18.7	.01
	4682	X -20.85	983	137.5 + 41.1 φ	38.31	4.6	0.979	13.8	.01
U	2885	-22.65		243 + 65.3 φ	68.32	4.1	0.88	12.2	.03
IC	467	X -21.41		114.7 + 40.4 φ	31.96	4.8	0.88	21.4	.01
	7541	B -22.14		150.8 + 123.5 φ	40.72	6	0.99	28.4	.02
	4321	X -21.62		177.7 + 44.7 φ	50.07	4.2	0.99	20.1	.02
	753	X -22.84		133.2 + 30.2 φ	56.84	3.9	0.61	44.6	.03
0	3691	-20.95	+.62	67.6 + 63.4 φ	18.1	7.4	0.99	14	.02
	1087	X -21.52		93.2 + 63.8 φ	25.34	3.5	0.31	19.4	.02
	4605	B -18.66		32. + 86.8 φ	8.29	4.2	0.98	4.3	.03
	2715	X -21.35		106.2 + 50.2 φ	29.29	5.5	0.66	20.2	.03
	7664	? -22.15		190.8 - 13.25 φ	45.64	4.1	0.98	34.9	.04
	701	B -20.48		61.5 + 179.5 φ	16.15	9.3	0.98	12.7	.02

we get

$$\bar{V} = V\left[1 - 2^{-1/2}\left(1 + \frac{R}{V}\frac{dV}{dR}\right)^{1/2}\right] \qquad (4.1)$$

From our fit we set

$$V(\varrho) = V_0 + V_1\varrho \qquad \varrho = R/R_{25} \qquad (4.2)$$

where R_{25} is the radius defined in CHAP I . Regardless of the slope in (4.2) we obtained that $\bar{V}$ is pratically (within very few percents) constant over the whole radius.

The actual values of $\bar{V}, V_0, V_1$ and z for each galaxy are listed in table 4 ; we also give same examples of the behaviour of $\bar{V}$ in figure 10

Links of $\bar{V}$ to the m/L ratio .

From (4.1) and because it is

$$V^2 = R\frac{\partial\phi}{\partial R} \qquad (4.3)$$

$$K^2 = \frac{3}{R}\frac{\partial\phi}{\partial R} + \frac{\partial^2\phi}{\partial R^2} \qquad (4.4)$$

upon substitution of (4) into (1) , since it is $d\bar{V}/dR = 0$, we obtain the following differential equation

$$R^2\frac{\partial^2\phi}{\partial R^2} + 3R\frac{\partial\phi}{\partial R} - 4(V - \bar{V}) = 0 \qquad (4.5)$$

where ϕ is the axisymmetric gravitational potential.

FIG 10

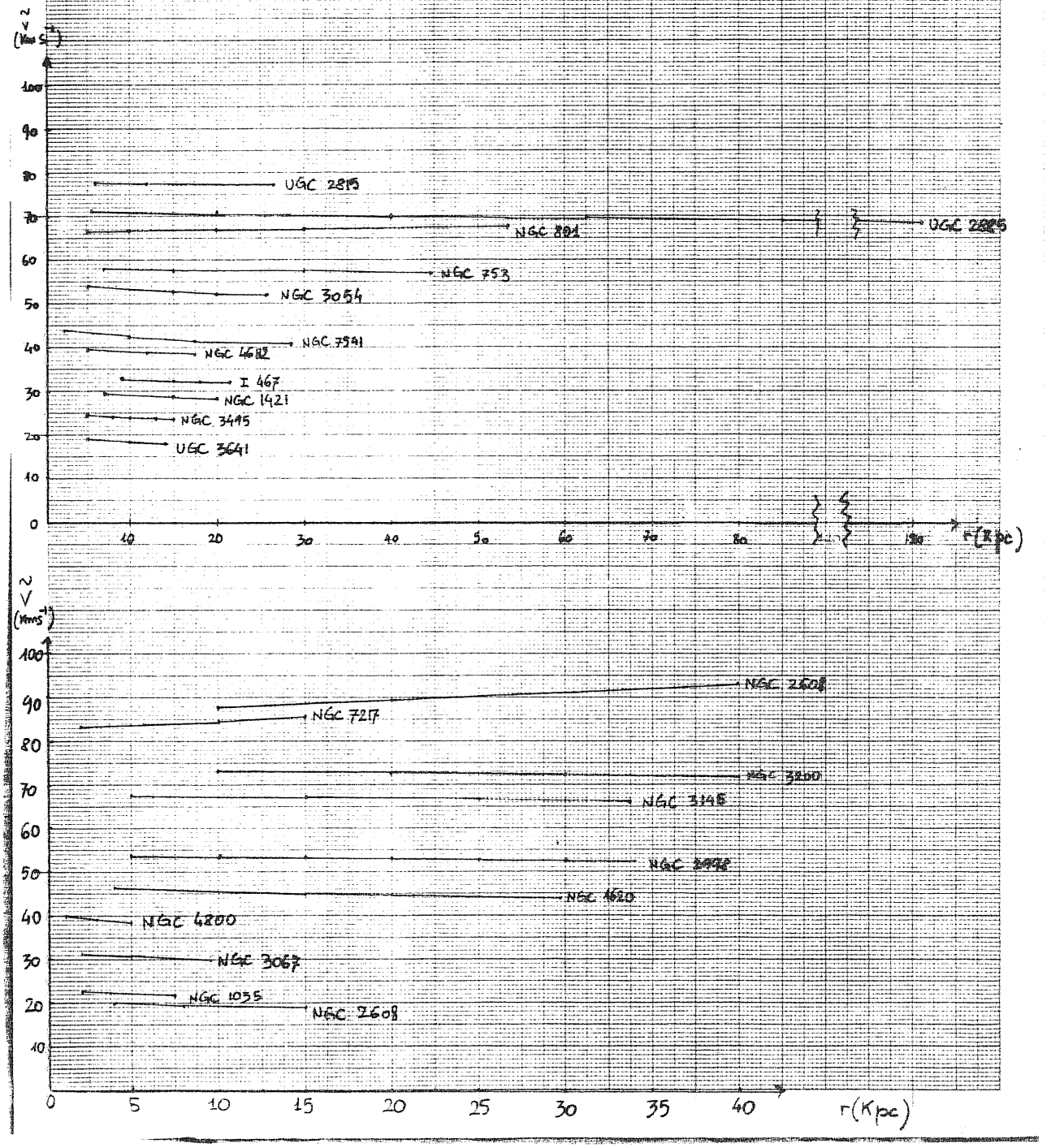
V² (Km S⁻¹)²
UGC 2885
NGC 801
NGC 753
NGC 3054
NGC 7541
NGC 4682
I 467
NGC 1421
NGC 3495
UGC 3641
r(Kpc)
NGC 2608
NGC 7217
NGC 3200
NGC 3198
NGC 4620
NGC 4200
NGC 3067
NGC 1035
NGC 2608
r(Kpc)

We note that the differential equation just written "carries" the gravitational potential in each galaxy and at the same time ,considering $\tilde{V}$ a dynamical parameter wich characterize the single galaxies,it describes the gravitational potential in all spirals.

Modelling galaxies as spheres,we couple (4.5) with the Poisson equation in spherical coordinates to obtain the mass as a function of V and of $\tilde{V}$. We get:

$$m(R_{25}) = G^{-1}\int_0^{R_{25}}(3V^2 - 8V\tilde{V} + 4\tilde{V}^2)dR = [3V_0^2 + 4\tilde{V}^2 + 3V_0V_1 + V_1^2 - 8\tilde{V}V_0 - 4\tilde{V}V_1]R_{25}G^{-1}$$
$$\cong G^{-1}V^2(R_{25})\,R_{25} \qquad (4.6)$$

We wish to stress that:

$$m(R_{25}) = m(\tilde{V}, V) \qquad (4.7)$$

We also point out in (4.7) that,even when the explicit and implicit through V^2 dependence on V_1/V_0 are small, the dipendence on V_1/V_0 through $\tilde{V}$ can be important.

Nevertheless , if we are interested in the general behaviour of the morphological classes rather than of the individuals,because $\langle V_1/V_0 \rangle \sim 0.4$,we are allowed to write

$$m(R_{25}) = G^{-1}\{3V^2 - 8V\tilde{V} + 4\tilde{V}^2\}_{R_{25}} \qquad (4.8)$$

One of the most important results of Rubin et al. is that they found a relationship between the circular velocity and and the luminosity within R_{25} . Similarly we obtain:

$$M_B = a_{\tilde{V}} + b_{\tilde{V}} \log \tilde{V} \qquad (4.9) \qquad M_B = a_V + b_V \log V \quad \text{from [ ]} \qquad (4.11)$$

$$\log R_{25} = a_R + b_R \log \tilde{V} \qquad (4.10)$$

where the actual values of $a_{\tilde{V}}, b_{\tilde{V}}, a_R, b_R$ are given ,togheter with their uncertainty and the correlation parameters of the fits in figure (10) for both Sb and Sc classes.

From (6.9) and (4.10/11) we obtain

$$\log\left(\frac{m}{L}\right) = \log\left[3\times 10^{2\left(\frac{M_B - a_V}{b_V}\right)} - 8\times 10^{\left(\frac{M_B - a_V}{b_V}\right)} 10^{\left(\frac{M_B - a_V}{b_V}\right)} + 4\times 10^{2\left(\frac{M_B - a_V}{b_V}\right)}\right] +$$

$$+ \log L_\odot + \log\left[a_R + b_R\left(\frac{M_B - a_V}{b_V}\right)\right] - \log G - 0.4\,(M_\odot - M_B) \qquad (4.12)$$

From the expression (4.12) we find the existence of a lim-t ting blue absolute magnitude $M_B \simeq -23.3$

This is in good agreement with current observational estimates.

Substituing in eq. 1.5 $V = V(L)$ we get a differential equation linking the paramount dynamical quantity to the luminosity.

Link of $\tilde{V}$ to the locations of resonances

Once we have the rotation curves it is possible to obtain R_i, R_e, R_c, if Ω_p is known, through the following relations

$$\Omega_p = \Omega(R_c)$$
$$\Omega - \kappa/2\big|_{R_i} = \Omega_p \qquad (4.13)$$
$$\Omega + \kappa/2\big|_{R_e} = \Omega_p$$

Nevertheless, when $V = \sum V_n \varsigma^n$ $\varsigma = R/R_{cs}$ ($\sim$ high), and above all if $\tilde{V}$ were not a constant, the resonance radii would connected to the background dynamical quantity (e.g. V) and to each other in a rather complicated way.

But, since in the present work we have $\tilde{V}$ const. and

$V = V_0 + V_1 R$ we get straight ahead

$$R_i = \frac{\tilde{V}}{V_0 + V_1 R_c} R_c$$

$$R_e = \frac{2V_0 - \tilde{V}}{V_0 - V_1 R_c} R_c \qquad (4.14)$$

$$R_c = \frac{V_0}{R_p - V_1}$$

A straightforward application of the formulae (4.14) can be done for those galawies which show inner (pseudo) rings [29] generally considered as the manifestation of the dispersion rings of the inner Lindbad resonances (De Vaucoleurs and Buta, 1983).

The results are shown in table 5

The galaxy NGC 7217 deserves a particular attention. It presents three rings, two inner and one outer. As shown in Table 5 the coincidence of the three rings with the predicted locations of the three resonance regions is striking.

Specific angular momentum and morphological types

An application to results obtained is to test,

the intuitive idea that late morphological types have available more specific angular momentum that the early types ones. Then the quantity j/m where j is the specific angular momentum, probably plays a role in the amplification of the responce (in terms of morphology) to a given spiral perturbation. In fact we espect that, for a given spiral-perturbation amplitude, the higher is the value of j/m the larger are the "visible" manifestations of that perturbing potential.

By working out j/m we derive a strong support to this idea,

TABLE : PARAMETERS OF SPIRAL STRUCTURE IN RING GALAXIES

NGC	R_i (Kpc)	R_c	$R_{footfoot}$	R_e	R_H	Ω_p (Km s^{-1} Kpc^{-1})	NOTES
753	7.7	26.7	24.7	52.3	44.6	7.4	$R_c \simeq R_f$ $R_e > R_H$
2715	3.7	19.6	18.4	36.9	20.2	7.9	$R_c \approx R_f$ $R_e > R_H \sim R_c$
2998	5.0	19.5	34.0	34.4	40.0	10.6	$R_c < R_f$ $R_e \simeq R_f \approx R_H$
3054	4.6	22.3	22.8	41.5	25.7	11.4	$R_c \approx R_f$ $R_e > R_H$
3145	7.6	38.8	25.4	53.3	33.8	8.7	$R_c \approx R_f$ $R_e > R_H \sim R_c$
3672	3.8	14.3	17.8	25.1	18.7	13.3	$R_c > R_f$ $R_e > R_H \sim R_c$
4321	5.5	25.8	14.6	47.6	20.1	17.0	$R_c > R_f$ $R_e > R_H \sim R_c$
7171	5.4	22.3	15.0	41.3	23.9	9.1	** SUPERPOSITION **
7217	1.2	4.2 (ring at 4.0 Kpc)	10.5	7.2 (ring at 9.1 Kpc)	15.1	68.0	$R_c \simeq R_H \simeq R_f$

as is shown in Figure 11 There is in facts a one-to-one increasing corrispondence between the values of J/M and the De Vaucouleurs T morphogical types.

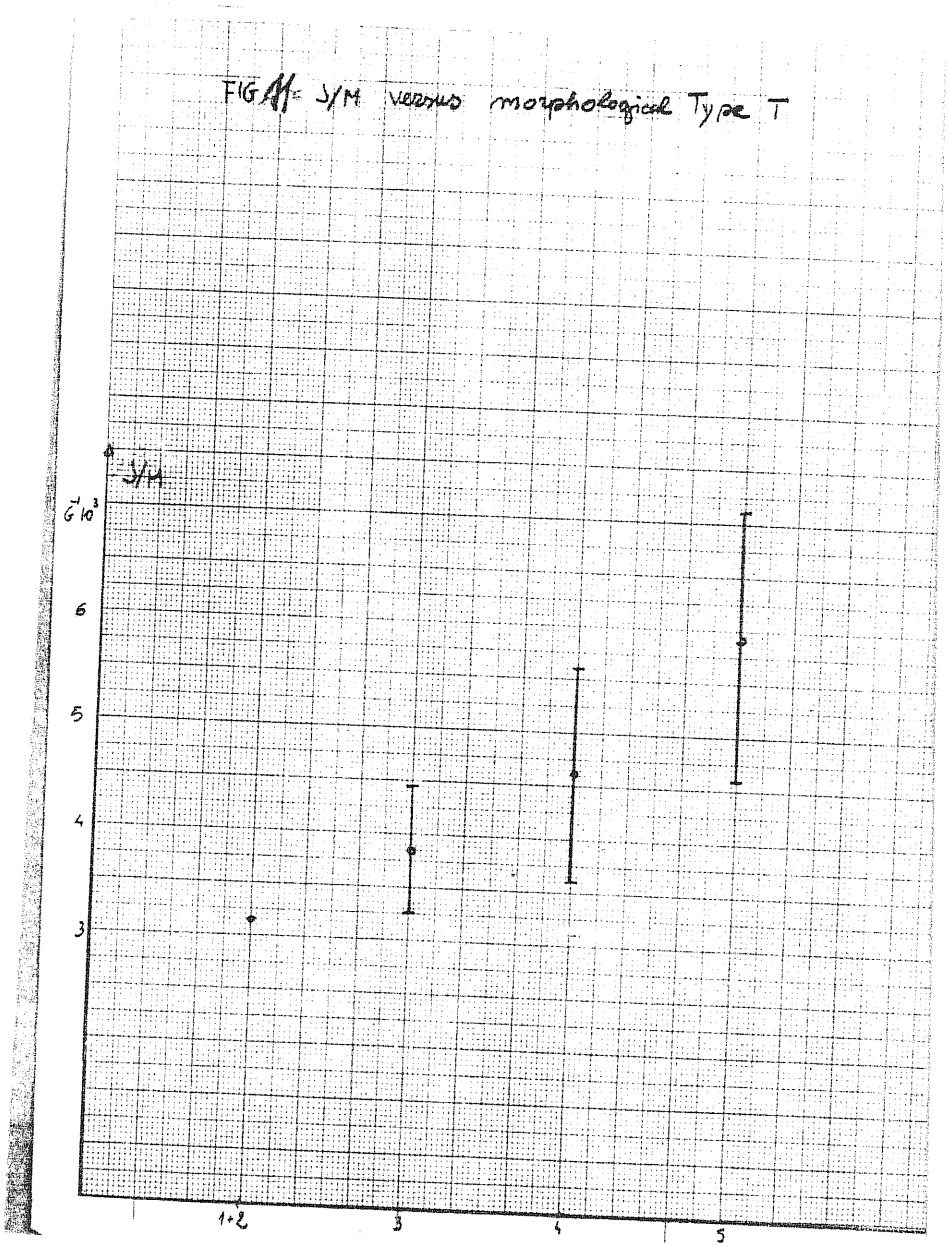

CONCLUSIONS

In these short review we pointed out:

1) the presence of dark haloes seems undoubteful, nevertheless all its consequences haven't been investigated yet.

2) Consequently we have to take care, interpreting rotation curves, of their slope.

3) Locations of resonances and pattern speeds are difficult to obtain too; we can know them only with a careful analisis of internal dynamics.

Let's remember that interesting theories of formation and survival of spiral structures have as groun the existence of resonances.

4) Galaxies are formed by several components; nevertheless there is no their track in the rotation: curves.

This loss of independency of different components, probabily is due to some mechanism coupling them.

5) This could be related to the fact that the linear velocity of the kinematical bisymmetrical perturbation $\tilde{v} = (\Omega - K/2)R$ keeps constant over the whole galaxy and represents it better than any other quantity: we can work out good dependency of $\tilde{v}$ on Luminosity and radius R_{25} of a galaxy.

AKNOWLEDGEMENTS

Thanks are due to Professor De Felice and to Dr. J. Miller for teir help and continue assistence.

Most of results presented in chapter 4 are obtained in frendly collaboration with Dr. M. Persic.

REFERENCES

(1) R.H. Berman, J.W.K. Mark, Ap.J. 216,257. (1977)

(2) R.H. Berman, J.W.K. Mark, Ap.J. 231,388. (1979)

(3) F. Hohl, Ap.J.168, 343. (1971)

(4) F. Hohl, Astron. J. 81, 30 (1976)

(5) C.C. Lin, F.H. Shu, Ap.J. 140, 646 (1964)

(6) D. Lynden-bell , A.J. Kalnajs MNRAS 157 ,1 .(1972)

(7) J.W.K. Mark Ap.J. 205 ,363. (1976)

(8)J.W.K. Mark Ap.J. 206 ,418. (1976)

(9) J.W.K. Mark Ap.J 212 ,645. (1977)

(10) J.P. Ostriker , P.J.E. Peebles
Ap.J. 186, 467. (1973)

(11) V.C. Rubin ,W.K. Ford ,N. Thonnard
Ap.J. 238 ,471. (1980)

(12) F.H. Shu Ap.J. 160 ,89. (1970)

(13) F.H. Shu Ap.J. 160 ,99. (1970)

(14) A. Toomre Ap.J. 138 ,385. (1963)

(15) A. Toomre Ap.J. 139 ,1217.(1964)

(16) A. Toomre Ap.J. 158 ,899. (1969)

(17) J.A. Sellwood, A.A. 99 , 362. (1981)

(18) A. Ambastha, R.K. Varma Ap. J. 264 , 413. (1983)

(19) A. Bosma A.J. 86, 1791. (1981)

(20) J.A.R. Caldwell, J.P. Ostriker Ap. J. 251, 61. (1981)

(21) P. Goldreich, S. Tremaine — Ap.J. 222, 850. (1978)

(22) A. Toomre — Ann. Rev. Astron. Astrophisic 15, 437. (1977)

(23) G. Bertin — A.A. 145, 127. (1983)

(24) J. Kormendy, C.A. Norman — Ap.J. 233, 539. (1979)

(25) K.C. Freeman — Ap.J. 160, 811. (1970)

(26) R.H. Miller, K.H. Prendergast, W.J. Quirk — Ap.J. 161, 903. (1970)

(27) W.J. Quirk — Ap.J. 167 , 7. (1971)

(28) W.W. Roberts ,M.S. Roberts ,F.H. Shu — Ap.J. 196,381. (1975)

(29) G. de Vaucoulers ,R. Buta — A.J. 83,637. (1980)

(30) G. Eftastiou , G Fall — MNRAS 193 189 (1980)

(31) V. Rubin , W.K. Ford, N. Thonnard — A.P.J. 261, 439 (1982)

(32) V. Rubin, W. K. Ford, N. Thonnard — APJ.L. 225 L117 (1978)

(33) M. Persic, P. Salucci — IN PREPARATION